Common Proper-Motion Halo Stars

by

John Pearson Sharkey

Submitted to

The University of Hertfordshire

in partial fulfilment of the requirements for the degree of

MSc by Research

Centre for Astrophysics Research

School of Physics, Astronomy and Mathematics

The University of Hertfordshire

July 2015

Abstract

Using the PPMXL proper-motion catalogue we have attempted to compile our own catalogue of common-proper-motion halo candidates, for use in a study of the difference in the lower end of the metallicity distribution of Globular clusters $[Fe/H] = -2.4$ and single field stars $[Fe/H] = -4.1$. This was achieved by tailoring several selection criteria based on the expected characteristics of typical halo stars, such as similar proper-motions and reduced proper motion data, and applying them to the chosen proper-motion catalogue. The final selection criteria produced a catalogue of 17,500 common proper-motion (CPM) halo binary candidates, and have been further refined to 2,326 pairs based on conclusions drawn from our analysis of the larger catalogue, and have shown that several pre-existing CPM halo binaries are included in the catalogue. A selection of 528 pairs has been identified from this final catalogue as having an increased likelihood over the larger catalogue of being CPM binary pairs.

A large number of issues have been identified with the PPMXL catalogue; chiefly among them is the large proportion of data that has been found to be spurious, caused in part by methods used in the creation of the original catalogue, which are discussed in this study. Additional faults found with the final catalogue lead us to the conclusion during the project that the data was of insufficient quality for the planned study on the metallicity distribution; however the refined catalogue and especially the 528 high-interest pairs are likely good candidates for finding real, wide halo binaries. Instead, identification of numerous problems found in the United States Naval Observatory, USNO-B1, catalogue and discussion of their likely causes has been performed.

A sample of 600,000 stars were found that share the characteristics of halo giants, though it is demonstrated that a large number of these are likely foreground disk stars.

Contents

1.0   Introduction

The primary goal of my project was to compile a catalogue of halo common proper-motion (CPM) pairs from existing catalogues of stars. The intention was for the catalogue to be used to investigate how the metallicity distribution of these pairs compares to that of single field stars and globular clusters; with a specific focus on pairs in the metal-poor end of the distribution. Because of this, the methods used to select stars for the catalogue have a bias towards the low metallicity end of the distribution.

A metallicity distribution curve shows what proportions of a selection of stars (such as globular clusters or whole galaxies) have a particular metallicity (typically the relative abundance of iron and hydrogen). These distributions can be used to test different theories of galactic evolution and formation; with the low end of the distribution giving details about the earliest era of star formation in the galaxy, including the mass function of the earliest stars, the extent of chemical pre-enrichment and the rates and yields of core collapse supernovae (Schlesinger et al., 2012).

One of the primary goals with the catalogue was to compare the metallicities of the most metal poor stars found in Globular clusters, field stars, and the CPM binaries of our catalogue, and see if there is any relationship. Currently, the metallicity distribution of globular clusters goes as low as roughly $[Fe/H] = -2.4$ (Kraft & Ivans, 2003), however, field stars can be found to around $[Fe/H] = -4.1$ (Yong et al., 2012). It is possible that the difference in the distributions could be due to globular clusters being unable to form at such low metallicities, or that there simply aren't enough of them to have found such a metal-poor example as the field stars. Comparing these stars with the lowest metallicity pairs from our catalogue may provide some insight into the differences, as an estimate for the metal-poor distribution of the halo is $[Fe/H] \leq -3$ (Tissera & Scannapieco, 2014) which will be of use for the comparison.

1.1   Halo Stars

The majority of the stars in the galaxy are located either close to the Galactic plane (the disk) or around the Galactic core (the bulge); a small minority of stars are found outside of these areas, in the Galactic halo. These stars are roughly split into two groups, Population I and Population II, based roughly on their ages and metallicities.

Population I are young, metal-rich stars, typically found in the disk and bulge of the galaxy, with low relative velocities and regular elliptical orbits. They typically have ages between $0 - 10$ billions years (Strobel, 2013), a mean velocity (relative to the sun) of 17 kms^{-1} (Blaauw, 1999) and metallicities anywhere between $0.1\ Z_{\odot}$ and $2.5\ Z_{\odot}$ (Strobel, 2013) (where $Z_{\odot} = 0.0122$, (Asplund et al., 2006)).

Population II stars are much older, more metal-poor stars, typically found in the Galactic halo. These stars tend of have highly elliptical and randomly aligned orbits. Their ages range between $10 - 13$ billion years (Strobel, 2013), with velocities typically > 75 kms^{-1} (Blaauw, 1999) and low metallicities of $Z < 0.01\ Z_{\odot}$ (Strobel, 2013).

Population II/halo stars, the focus of this study, can most easily be separated from the stars found in the disk and bulge by their much greater proper-motions which arise because of the considerable difference between the typical velocity (speed and direction) of Population I stars on the one hand, and Population II stars on the other, as detailed above; and so the use of proper-motion catalogues will likely be the first step taken in identifying these stars.

1.2   Motivation

While not within the scope of the project, due to time constraints and a predetermined direction for the project, some possible uses for a catalogue of common proper-motion pairs include:

- Constraining the dark matter content of the Milky Way (Quinn et al. 2010), where very wide binary halo stars are useful because of their ages, which means they are less affected by the disruptive effects of stellar and Giant Molecular Cloud encounters than similar stars found in the disk. Existence of these very wide binary halo stars can be used to constrain proposed limits on the dark matter content of the Milky Way, as these binaries would not exist at a larger mass.

- Investigating lithium processing in cool, metal-poor halo dwarfs (Ryan & Deliyannis, 1998). In this study, high resolution spectroscopy is used to measure the lithium abundances of stars cooler than the Spite plateau, which can then be used to help understand which mechanisms may also affect stars on the plateau. This clarifies the relationship between the lithium abundances of warmer halo stars and the primordial value, which constrains the baryon density of the universe.

- Determining the dynamical and merger history of our galaxy (Allen et al., 2007). Wide and fragile halo binaries are likely to be the remains of past mergers or of dissolved clusters and should show up in the distribution of old stars, as coherent tidal streams, tails and moving clusters. These remnants can be identified by similar motions and metallicities found in groups of halo stars.

1.3   Catalogue Requirements

There are several requirements needed to successfully identify accurate CPM halo star candidates. The catalogue(s) chosen for the project must contain both accurate astrometry and photometry.

- Accurate positions are required to determine whether candidate pairs are close enough physically to be a binary system (though closeness in the sky is not sufficient to determine whether the pair are actually related),

- o Positions in the catalogues considered for the project are typically accurate to between $100 - 200$ mas.

- Proper-motions for each star are required to determine whether they are moving together ('common' proper-motion),

  - o Proper-motions in the catalogues considered for the project were typically accurate to between $8 - 20$ mas/yr^{-1}

- Precise photometry is needed in combination with the proper-motions to create RPM diagrams (discussed in 3.2) which will allow halo stars to be separated from disk stars.

- Though brightness should be a consideration for future spectroscopy work, it was decided that no limit would be imposed for the initial catalogue to allow all possible stars, with the intention of then later sorting out for which stars reliable spectroscopy could be obtained. A quick estimate for what may be required would be $i = 18$ for intermediate resolution and $i = 15$ for high resolution.

- Specific optical/NIR colours could have been a requirement, though we chose to allow any passbands as long as they were reliable, as quality is required for further study. NIR may be more desirable as it is less affected by reddening, though this is not a limiting factor, particularly for halo stars away from the Galactic plane.

- We require that a catalogue goes deep enough to include the spectroscopic limits mentioned above

- The catalogue's completeness was not much of a consideration for the project as we only require a sample of CPM stars. It is not important that we obtain all possible sources at high proper-motions or faint magnitudes.

2.0   Background

2.1   Proper-motion Catalogues

To compile a catalogue of stars with common proper-motions we chose to make use of existing proper-motion catalogues. Short summaries and comments on the catalogues considered are included here.

2.1.1   LHS Catalogue

The Luyten Half Second (LHS) catalogue contains the positions, proper-motions and photographic magnitudes for roughly 4500 sources having proper-motions above $0.5^{"} \text{yr}^{-1}$ (Luyten, 1979a). The catalogue makes use of 804 fields from the Bruce Proper Motion Survey, which were hand-blinked or processed by an automatic blink-machine to identify high proper-motion sources. The catalogues positional errors are typically greater than $10^{"}$.

There is a revised version of the catalogue available which includes improved positions and proper-motions for almost all of the original sources using digital scans of the Palomar Sky Survey (POSS I and POSS II) plates (Bakos et al., 2002). The new positional accuracy is between $2^{"}$ and $8^{"}$ and the accuracies of the proper-motions are given as $0.1^{"} \text{yr}^{-1}$. For ~ 800 of the catalogues sources that could be identified in the TYCHO-2 and Hipparcos catalogues, positions and proper motions were replaced with these more accurate data.

The precision of the proper-motions and photometry of the original LHS catalogue are not available, however due to the fact that the New Luyten Two Tenths (NLTT) catalogue (See Ch. 2.1.2) was compiled from the same plate material as LHS, by the same person, the two catalogues would be expected to have similar levels of accuracy. Additionally, as the catalogue was produced in 1979, they are likely to be less accurate than more recent catalogues due to

improved methods of obtaining accurate proper-motions of sources (e.g. calculating absolute proper-motions rather than apparent).

This catalogue was not chosen for the current study based on more recent catalogues, such as rNLTT, having both an increased number of sources and more accurate data due to more sensitive equipment and improved methods.

2.1.2 The NLTT and rNLTT Catalogues

The New Luyten Two Tenths (NLTT) catalogue is an all-sky high-proper-motion catalogue of sources with relative proper-motions above $0.18^{"}\mathrm{yr}^{-1}$(Luyten, 1979b). The catalogue contains roughly 59,000 sources and extends down to a magnitude of $V \approx 19$. However, the catalogue is only complete to a magnitude of $V \approx 11.5$ where $|b| > 15$ and is stated to drop to $\sim 75\%$ near the Galactic plane (Luyten, 1979b).

A revised version of the catalogue exists, rNLTT, using improved positions and proper-motions for the ~36,000 sources present in the overlap between the POSS I and the second Two Micron All Sky Survey (2MASS) data release (Salim & Gould, 2003). These improved positions are given as being accurate to 130 mas at J2000 and proper-motions to 5.5 mas yr^{-1}.

Chanamé & Gould (2004) identified a problem with CPM pairs identified by Luyten while creating the original NLTT catalogue. For any stars Luyten determined to be a CPM binary, independent proper-motions were not recorded; instead, both stars were given the same proper-motion. In the revised catalogue, Chanamé and Gould chose to attempt to identify and verify sources in NLTT which were indicated as being a component in binary or multiple systems by searching a $1°$ radius around each source. If possible, improved proper-motions from PPM or USNO were included to make decisions as to whether identified sources were companions. This resulted in 1,235 CPM binaries in the revised catalogue, compared with 2,400 given by Luyten.

Though it would still be possible to find pairs using this catalogue, I would not have been able to do some crucial future work, specifically, studying the proper-motion difference between the supposed pairs, nor pairs fainter or with lower proper motions than the NLTT and rNLTT limits.

The accuracy of the photometry in the NLTT catalogue was not readily available, but as it was created using the same plates as the LHS catalogue, at the same time and by the same person, they are expected to be similar to the LHS and therefore likely to be surpassed by more recent catalogues, which have been able to employ improved methods of extracting data from photographic plates, such as SUPERBLINK.

I decided not to use this catalogue, due to the number of sources being much lower and errors being improved upon in some of the more recent options and due to the problem identified regarding the CPM binary identification.

2.1.3 LSPM Catalogue

Lépine and Shara Proper Motion catalogue (LSPM) is a catalogue of roughly 62,000 sources north of the J2000 celestial equator with relative proper-motions above $0.15''\mathrm{yr}^{-1}$ (Lépine & Shara, 2005). The catalogue was generated using their own SUPERBLINK software to manually search the POSS I and POSS II plates for high-proper-motion sources. Where possible, optical magnitudes from TYCHO-2, photographic magnitudes from USNO-B1 and infrared magnitudes from 2MASS have been included in the catalogue. Positions in the catalogue are accurate to $\sim$100 mas at J2000 with absolute proper-motions (with an extragalactic reference frame) which have a given accuracy of $\sim$8 mas yr^{-1}.

The catalogue is estimated (Lépine & Shara, 2005) to be 99% complete at high galactic latitudes ($|b| > 15°$) and $\sim$90% at low galactic latitudes ($|b| < 15°$) down to a magnitude of $V = 19$.

While the accuracy of the data in the catalogue is good, the low number of sources compared to the following catalogues resulted in it not being chosen for our catalogue. However, it can be used later for checking proper-motion differences between catalogues

2.1.4 SuperCOSMOS

The SuperCOSMOS Sky Survey (SSS) was a project which aimed to scan the multicolour/multi-epoch Schmidt photographic atlas material to produce a digital survey of the whole sky in three colours (B, R and I) with one colour (R) in two epochs (Hambly et al., 2001a).

The absolute astrometric accuracy of the catalogue is typically 0.2" depending on position and passband and its proper-motions are given as being accurate to ~ 10 mas yr^{-1} (Hambly et al., 2001b)., which are similar to some of the more recent catalogues such as LSPM and USNO-B1.

The catalogue's photometry in any given passband is typically accurate to 0.3 mag at m > 15 with colours being extremely accurate at $\sigma_{B-R} \sim 0.07$ at $B_J \sim 16.5$. The catalogue is estimated to be close to 100% to within ~1.5 mag of the nominal plate limits and is shown to be $> 90\%$ complete to $B_J \sim 20.5$ (Hambly et al. 2001c).

2.1.5 USNO-B1

The United States Naval Observatory (USNO-B1) is an all-sky catalogue of roughly 1,000,000,000 sources, containing their positions, relative proper-motions and B, R and I photometry(Monet et al., 2003). The data were taken from scans of 7435 Schmidt plates from several sky surveys over a period of 50 years.

The J2000 positions provided by the catalogue are given as being accurate to 0.2". This accuracy is surpassed by other catalogues compiled at this time, such as LSPM, and is limited partly by to

the widely spread observations that make up the catalogue. The proper-motion errors in the catalogue are given as ranging between $4 - 20$ mas yr^{-1} and a photometric accuracy of 0.3 mag in up to five colours.

The catalogue claims to be complete down to $V = 21$, but this is shown to be incorrect depending on the proper-motion and brightness of the sources (Gould, 2003); this is mentioned below in the USNO-B1 caveats.

Though this catalogue provides the largest number of sources of the catalogues available, I decided not to use it based on several of the problems with the catalogue which are highlighted in the caveats below:

- The USNO-B1 catalogue was tested by Gould (2003) to determine the completeness at high proper-motions ($\mu > 180$ mas yr^{-1}). It was found that up to 99% of high-proper-motion sources in the catalogue were spurious. When the catalogue was constructed, all detections within $30^{"}$ of a source, where movement could be matched to straight-line motion over time, have been included. This is more noticeable at high proper-motions and gives rise to large numbers of false pairings between the first and second epoch plates, leading USNO-B1 to list sources with high proper-motions that are fictitious. For example, at high galactic latitudes, the catalogue provides 200 times more entries than rNLTT and LSPM (Gould, 2003), which are said to be complete down to $V \approx 19$. This contamination was deliberate, with the intention of allowing users to search through all possible associations and sort out the results for themselves (Gould, 2003). This problem became a large issue during the project, where we discovered that not only are some of the proper-motions fictitious, but also some of the objects; this will be discussed in greater detail in Ch. 4.4.4.

- Relative proper-motions in the catalogue were determined by assuming that the motions of certain objects (generally background galaxies) in each plate are zero. These objects are chosen because as they are quite distant, their proper-motions are naturally quite small. In contrast, absolute proper-motions are calculated using specific reference

objects, typically distant quasars, which are known to have negligible proper-motions, which give a more accurate representation of the source's actual proper-motion (Titov, 2010). Using relative proper-motions may lead to problems in the future if the differences between relative and absolute proper-motions are significant for any sources.

2.1.6 PPMXL

The Positions and Proper Motions XL (PPMXL) catalogue is a combination of the USNO-B1 and 2MASS catalogues in which the relative proper-motions of the USNO-B1 catalogue have been converted to absolute proper-motions in the International Celestial Reference System (ICRS) (Roeser et al., 2010). The catalogue contains the positions (J2000), absolute proper-motions and USNO-B1 photographic magnitudes for roughly 900 million sources, with 2MASS photometry for around 410 million of these.

The cross-matching process between 2MASS and USNO-B1 was performed by using a cone search with a 3 arcsec radius. Double (or in fact multiple) identifications were allowed during the process (Roeser et al., 2010), the consequences of which are mentioned in detail in the caveats below; and which, like the USNO-B1 fictitious proper-motions and identifications noted above (Ch. 2.1.4), became problematic in the present study.

If the cross-matching process was successful, 2MASS astrometry has been provided, giving positional errors of $80 - 120$ mas; if unsuccessful, USNO-B1 astrometry was used, resulting in positional errors of $150 - 300$ mas. The errors in proper-motion range from 4mas yr^{-1} to $> 10\text{mas yr}^{-1}$, but are tabulated separately for each source. PPMXL aimed to be complete down to $V \approx 20$.

Despite PPMXL having 10% fewer sources than USNO-B1, I have decided to use PPMXL for my work. It has slightly improved errors compared to USNO-B1, and has converted the relative proper-motions from that catalogue to absolute proper-motions. The inclusion of the 2MASS

photometry was expected to be a bonus which allows me to implement additional selection criteria to the initial catalogue before potentially introducing more accurate photometry from another catalogue.

There have been a number of problems that have been identified in PPMXL which are covered in the caveats below:

- As the PPMXL catalogue used data from the USNO-B1 catalogue, it inherits the problem with the spurious high-proper-motion sources mentioned in the USNO-B1 caveats. This problem can be partially countered by flagging especially high proper-motion sources and comparing them with those from other catalogues (rNLTT and LSPM).

- Ideally, cross-matching the 2MASS and USNO-B1 catalogues should result in a single entry; however this has only occurred for between $93.6 - 88.7\%$ of cases in the northern and southern hemispheres respectively. The remainder are double or multiple matches, which increase in frequency at plate boundaries and in dense regions (Galactic plane). It is estimated that 90 million entries (10%) are doubles or multiples from USNO-B1 and 6 million (1.5%) are doubles or multiples from 2MASS (Roeser et al. 2010). Because of this, it may be prudent to flag non-unique matches when analysing the final catalogue.

- As we were to discover in the analysis (Ch. 4), since double identifications with 2MASS were allowed when PPMXL was constructed, the assignment of 2MASS data does not constitute verification that a PPMXL source is genuine or even that the 2MASS photometry provided is a good match to the USNO-B1 source.

2.2   Photometric Catalogues

For the photometry needed to determine whether CPM stars are from the Galactic halo or not, two major photometric catalogues were considered, The Two Micron All Sky Survey (2MASS)

and the Sloan Digital Sky Survey (SDSS). Though some of the proper-motion catalogues discussed above include their own photometry, the precision of some of these measurements can be much improved by using a separate photometric catalogue. Short summaries of these catalogues are included here.

2.2.1 2MASS

The Two Micron All Sky Survey (2MASS) was an all-sky survey (99.998% coverage) undertaken by two telescopes in Arizona and Chile between 1997 and 2001, collecting data on roughly 470,000,000 sources in the near-infrared (J, H and K) bandpasses (Skrutskie et al., 2006). The photometric error is given as < 0.02 mag for bright sources (< 13.0 mag). The catalogue's astrometry is accurate to ≤ 100 mas relative to the Hipparcos reference frame at $K_S < 14$.

2MASS photometry has been included in the PPMXL catalogue for roughly half the sources, so this data can be used to implement some preliminary photometric criteria on the data which can potentially then be improved upon later using SDSS.

2.2.2 SDSS

The Sloan Digital Sky Survey (SDSS) is an in-depth survey of roughly a quarter of the sky (mostly in the Northern Hemisphere) taking place from 2000 to the present, producing roughly annual data releases (Ahn et al., 2012). The survey has been done in several colours (u, g, r, i and z) and also includes some spectroscopic data in some of its more recent data releases (Ahn et al. 2014).

The most recent data release is DR12 (July 2014), however at the time the catalogue was being considered, DR10 was the most recent. DR10 gives J2000 positional accuracies of $\sim 0.1''$ and photometric accuracies of 0.05 at $g = 18.0$ with much smaller errors for brighter sources. The catalogue claims to be 95% complete to roughly magnitude 22 in all colours. SDSS contains roughly 470 million sources of which 260 million are confirmed as being stars (Ahn et al. 2014).

It was originally planned to use this catalogue for the project, but due to complications, discussed later, the work did not advance far enough to make use of it.

2.3 Catalogue Interrogation Tools

The methods for interrogating catalogue data vary depending on whether the data is stored locally or accessed using an online service. If the data is stored locally; programs such as python or excel can be used to implement criteria on the catalogue to obtain the desired data. This has several benefits, as python is an incredibly versatile program which would allow a large range of criteria to be implemented at once. However the drawback in using these methods is that they require local computing power to run; which, depending on the criteria and catalogue size, could result in queries taking many hours to complete. It was therefore decided to use an online service, where selection criteria are submitted as a plain text query, and results are returned through the service, having used the service's computing power rather than our own. Two services were considered, and are discussed here.

2.3.1 Table Access Protocol

Table Access Protocol (TAP), produced by the International Virtual Observatory Alliance (IVOA)[1], is a service protocol that is used to access table data such as astronomical catalogues and databases. TAP can query databases in a number of query languages such as Astronomical Data Query Language (ADQL) and Parameterised Query Language (PQL). These languages are based on Structured Query Language (SQL), with ADQL having been produced specifically for use on astronomical catalogues. ADQL can be used to interrogate a catalogue through TAP by imposing search criteria in the form of logic statements and mathematical functions. To apply TAP

---

[1] http://www.ivoa.net/

queries on an online database, a service such as TAPHandle[2] must be used. This service has access to most astronomical catalogues including PPMXL and SDSS DR7.

For my project, TAPHandle was used to implement criteria to the whole PPMXL catalogue and return a subset containing only the stars we are interested in.

2.3.2   NASA/IPAC Infrared Science Archive

The Infrared Science Archive (IRSA) is a collection of National Aeronautics and Space Administration's (NASA) infrared and submillimetre missions, including many large-area and all-sky surveys. In total, IRSA provides access to more than 20 billion astronomical measurements, including the PPMXL catalogue.

This service can be queried in the same way TAPHandle is, allowing for criteria to be imposed on the data before it is received. IRSA also has several features that aren't available on TAPHandle such as preset cone, box and polygon search methods and optional output methods (including the ability to email finished results, which does not require a computer to remain active for the run time of the query, which can be several hours), all of which make the system much more convenient to use.

However, after attempting to use this service to compile my catalogue, it was found that some of the resulting data did not meet the criteria that had been imposed on it. When the criteria shown in Fig 2.1 were used with the service, the data demonstrated in Fig 2.2 were returned.

---

[2] saada.unistra.fr/taphandle/

Though the criteria explicitly states that the results should lay between the two lines in the figure, data can be found outside of the limits. An explanation for this was not found, and as the results from the service were found to be unreliable, TAPHandle was used for the study instead.

(abs(pmra/e_pmra)>4 or abs(pmde/e_pmde)>4)

and jmag is not null

and kmag is not null

and jmag+5*log(10,0.0000001+3600*power(pmra*pmra+pmde*pmde,0.5))+5<8 and jmag-kmag>0.47

and -4.854*(jmag-kmag)+10.281
<jmag+5*log(10,0.0000001+3600*power(pmra*pmra+pmde*pmde,0.5))+5

Figure 2.1   An early version of the selection criteria, which was imposed on the NASA/IPAC service. Most importantly, the last two lines impose limits on the reduced proper motion of the data.
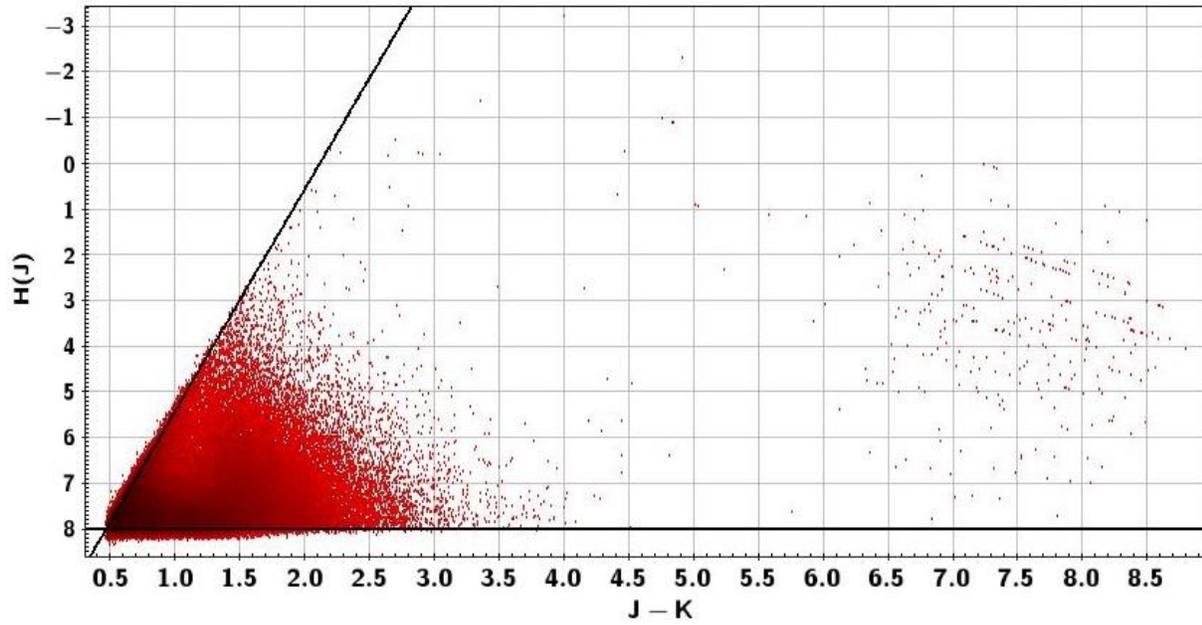
Figure 2.2   Data returned by NASA/IPAC service after imposing selection criteria given in Fig. 2.1. The black lines represent the limits which should have been adhered to, though some data are found outside these limits.

3.0   Selection Criteria Methodology

To retrieve appropriate and reliable candidates for our work, we needed criteria with which to interrogate the PPMXL catalogue, leaving us with only the sources we are interested in.

Using the TAPHandle service (Ch. 2.3.1), there are several selection criteria which we can impose on the PPMXL data, each of these are discussed in greater detail later.

As it was originally unknown what the best criteria for selecting the sources we required should be, each of the selection criteria had to be refined progressively. In making these refinements, there was a trade-off, in that inclusive criteria maximise the number of genuine binaries in the final catalogue but also increase the number of chance associations (erroneous binaries), which needed to be considered. The following chapter focuses primarily on the results of these refinements.

3.1 High Proper Motion

One of the features of halo stars is that they have large proper motions compared to disk stars, so the first criterion considered for implementation was to remove any sources that could not be confidently described as having a significant proper-motion.

As the PPMXL data include proper-motion errors for individual sources, it was decided that requiring each source to have a proper motion greater than a certain multiple ($Z)$ of the proper-motion error would be the first step to ensure that the published proper-motion values were statistically significant, i.e. not dominated by the measurement error.

To determine how many standard deviations our limit would be, a sample of 10,000 sources (from a region of sky I randomly selected by requesting 'TOP 10000' sources from PPMXL, the region is found between $56.09 < RA < 58.99$ and $22.16 < dec < 23.24$) was tested to find

what fraction of the sample remained after imposing various proper-motion limits, as shown in Figure 3.1.
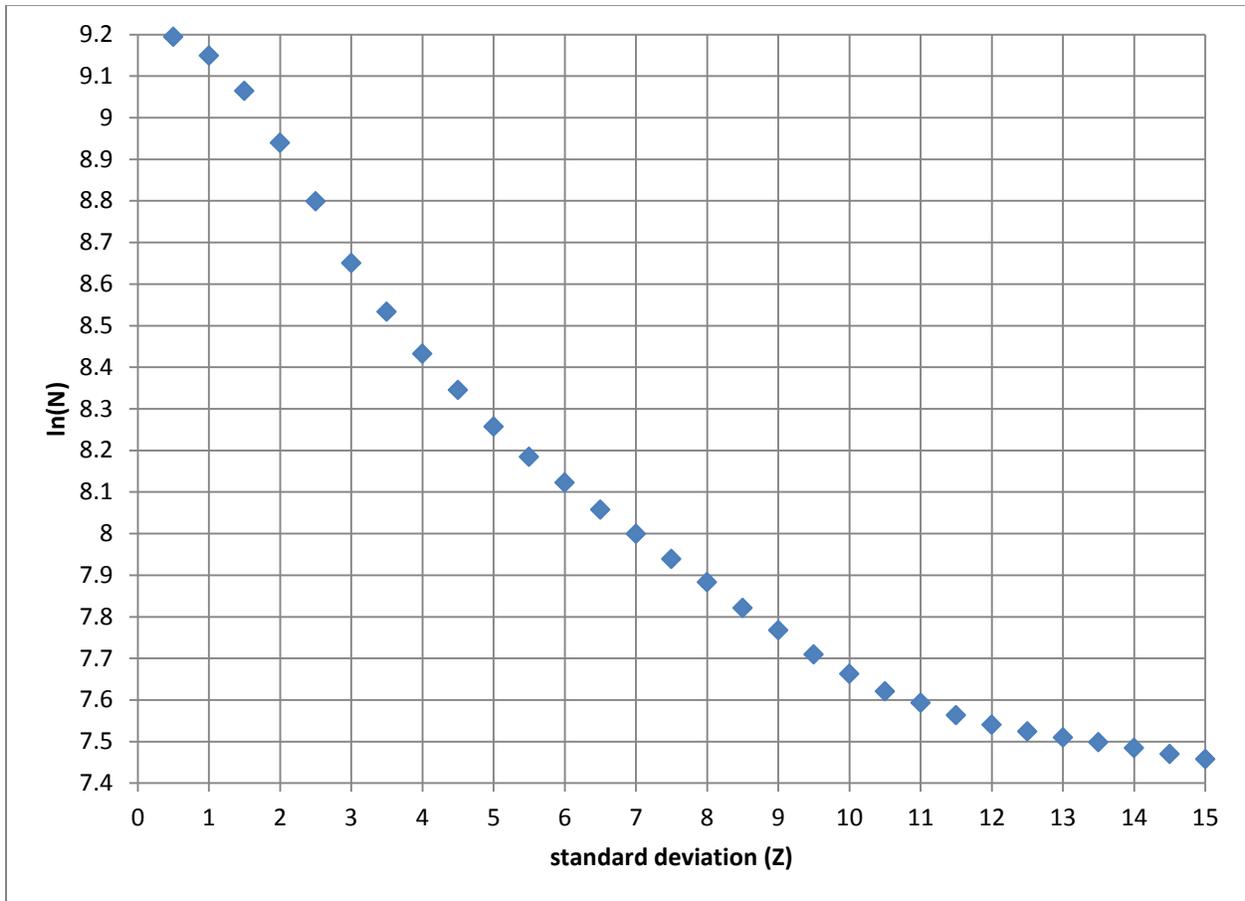
Figure 3.1: The number of catalogue sources, *N*, with total proper motions greater than *Z* times the proper-motion error. Note the log-linear scale; see text for interpretation.

If the proper-motions of the sources in the PPMXL catalogue were only due to Gaussian random errors, Figure 3.1 would appear as a Gaussian distribution (an inverted parabola in this log-linear plot). An inverted parabolic form can be seen in the plot at lower standard deviations $(Z < 3)$. It is evident that these sources would be unreliable, as their proper-motions cannot be distinguished from those caused by random errors. At roughly $Z = 4$, i.e. 4σ, the distribution exceeds the inverted parabola and begins to flatten out. We can be reasonably confident that sources above this point have proper-motions that are not due to Gaussian

errors and are therefore of use to the project. Based on the sample selected, imposing this criterion will return roughly 45% of the PPMXL catalogue.

For the final criteria however, it was determined that a lower limit of 5σ produced data which was more relevant to the project. It was found that with the 4σ criteria there was still a noticeable percentage of disk stars contaminating the results, and to attempt to remove as much of the contamination as possible, the criteria was made more strict. It is recognised that this criterion could be relaxed in future once genuine binaries are detected, and the utility of the adopted selection criteria has been verified.

For a Gaussian distribution, the chances of >2, >3 and >4 sigma outliers is $4.6\%, 0.27\%$ and 0.0064% respectively, so the majority of our sources should have genuine significant proper motions.

3.2   Reduced Proper-Motion and Colour Cuts

Reduced proper-motion (RPM, *H*) is a term which is used to relate the apparent magnitude, *m*, and proper-motion, μ, of a star with its absolute magnitude, *M*, and transverse velocity, $v_\perp$, (Stromberg, 1939).

$$H_V = m_V + 5\log_{10}(\mu) + 5 \tag{3.1}$$

which by introducing the distance modulus, $m - M = 5\log_{10}(d) - 5,$ and recognising that $v_\perp = 4.74\mu d \quad \text{kms}^{-1}$ (where μ is in arcsec and d is in parsec), can be written as;

$$H_V = M_V + 5\log_{10}(v_\perp) - 3.37 \tag{3.2}$$

Reduced proper-motion was first introduced by Hertzsprung (Hertzsprung, 1905) though the symbol H for the term was first used by Luyten (Luyten, 1922a). Luyten had previously used a different notation (M_μ) in an earlier paper (Luyten, 1922b) and switched to 'H' that year; possibly in recognition of Hertzsprung's earlier use.

As can be seen from Equation 3.2, an RPM diagram, RPM (H) against a colour index, e.g. (J-K) is similar to a colour-absolute-magnitude diagram (HR diagram) M vs J-K, but stars' stellar evolutionary tracks and isochrones plotted on it are displaced according to their transverse velocities (Eq. 3.2). These diagrams can be used to separate the typically fast moving halo stars from the relatively slow moving disk stars and allows us to identify the evolutionary phases of these stars.

To identify and separate the desired stars from this diagram, portions of the diagram are selected using cuts, though this requires accurate photometry to give confident results.

USNO-B1 photometry is included for all sources in the PPMXL catalogue for at least one of the USNO-B1 bandpasses; though, for the majority of sources, many USNO-B1 bandpasses are missing. The 2MASS data (JHK photometry), included for roughly half the sources, are much more accurate than that of USNO-B1 (see Ch. 2.2.1) and each includes all three bandpasses used in the catalogue. For these reasons, the J and K colours have been used to make cuts to the data, however it should be noted that this decision instantly removes half of the PPMXL catalogue. The b2 magnitude distribution is included in Fig. 3.2 for the stars that are lacking 2MASS data.
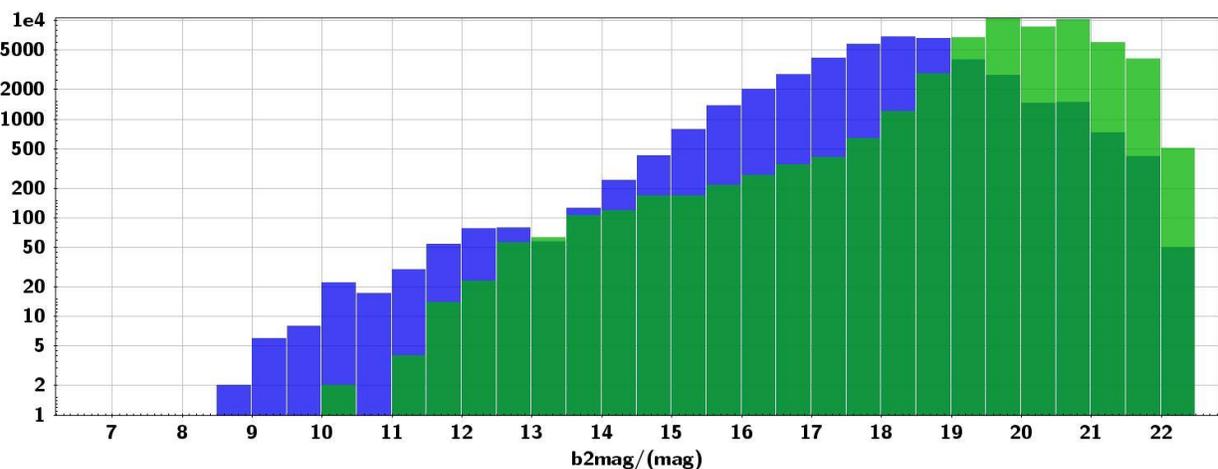
Figure 3.2   B2 magnitude distribution for ~55,000 sources without 2MASS data in green and ~45,000 with 2MASS data in blue (From a sample of top 100,000 sources from the PPMXL catalogue, in the region $136.99 < RA < 141.33$ and $-40.65 < dec < -37.70$.

An estimate for the age, mass and transverse velocity of a typical main sequence halo star at the main sequence turnoff would be $\sim 12\,\mathrm{Gyr}$ (Jofré & Weiss, 2011), $\sim 0.8\ M_\odot$ (Bertelli et al., 2008) and $\sim 200\ \mathrm{km\ s^{-1}}$ (Gould, 2003).

Using a Padova isochrone (Bertelli et al., 2008), for $\log_{10}(\mathrm{Age/yr}) = 10.05$ and $Z = 0.0001$ (as the planned future work desired a focus on low metallicity halo stars, and this was the lowest metallicity Padova isochrone available) the RPM in the J bandpass for the 'typical' halo star was calculated, as shown in Figure 3.3.

The main sequence of this isochrone, shown in Figure 3.3, was approximated as $H_J(200\ \mathrm{km\ s^{-1}}) = 9.6(J - K) + 9$. Only sources below this line have been included in the final catalogue, as sources above this point are more likely to be disk stars.

Additionally, colour limits of $0.15 < (J - K) < 0.65$ were created based on the figure (and are indicated by the blue lines). The upper limit was chosen as it was expected that any sources above this limit would be difficult to work with and perform follow up spectroscopy on as they are faint and have a lot of spectral lines making them harder to analyse. In hindsight, the lower limit could have been made to be a better fit (possibly $J - K > 0.23$), to the main-sequence turn off indicated in the figure; however at the time, it was preferential to include more possible pairs and refine them later, and the lower limit has the chance to pick up any blue stragglers (main sequence stars in a cluster that are more luminous and bluer than stars at the main-sequence turn-off point of the cluster (Sandage, 1953)) which may be found in the data.
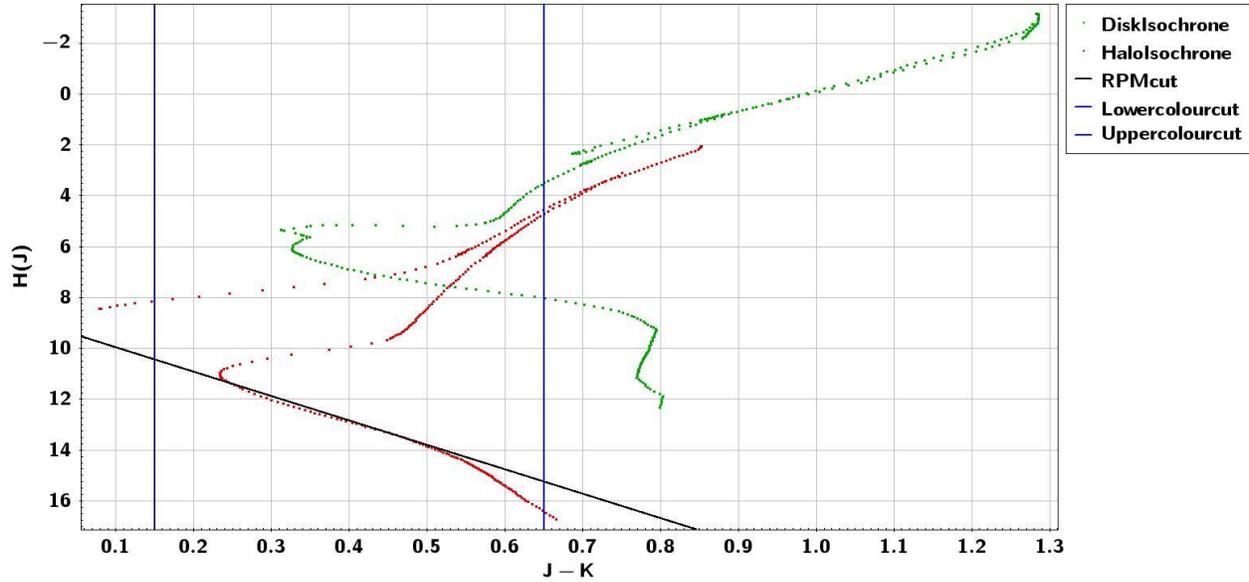
Figure 3.3: Padova isochrones for a typical halo star (Z=0.0001, age=12 Gyr, $v_\perp = 200 \text{ kms}^{-1}$) and a typical disk star ($Z = 0.0017$, $age = 5$ Gyr, $v_\perp = 20 \text{ kms}^{-1}$) in a reduced-proper-motion diagram with a linear approximation to the halo stars' main sequence.

3.3   Proper-Motion Difference

For any pair of stars to be declared a CPM binary, their proper-motions are required to be quite similar to each other. Differences between the individual proper-motions can have two causes, errors in the measurements, and the orbital motion of a genuine pair.

Depending on the distance to the pair, their masses and the angle of their orbit, the orbital motion can have a large effect on the proper-motion difference between the two stars. However, as our catalogue is focusing on halo stars, the large distances to our stars mean that proper-motion difference due to orbital motion should be small, especially compared to those caused by errors in measurement. This expectation was confirmed, with the benefit of hindsight, once the final catalogue was selected, and the analysis is briefly set out here, even though the final catalogue has not yet been presented

Using the Padova isochrones from Ch. 3.2, estimates for absolute J magnitudes were produced for J-K values from the catalogue based on a linear approximation of the main sequence ($J = 9.6(J - K) + 1$), as shown in Fig. 3.3.

The distance modulus, $m - M = 5\log_{10}(d) - 5$, can then be used to give estimates for the distance to each source in the catalogue. As will be shown later in the thesis, the application of the full set of selection criteria (which I have yet to introduce) gives rise to a catalogue with an average distance found to be $\sim$500 pc.

The angular separation (in degrees) between the two stars of the pair was calculated using;

$$Separation^2 = \Delta\delta^2 + (\Delta\alpha \times \cos(\delta))^2 \qquad (3.3)$$

where α and δ (right ascension and declination) are both given in degrees.

Using the distances and angular separations, physical separations can be determined for each pair, and then used to calculate the orbital velocities of the binary systems ($M = 0.8M_\odot$ for a typical halo star).

$$v = \sqrt{\frac{GM}{r}} \qquad (3.4)$$

The average orbital velocity of the binary systems in the final catalogue was found to be 0.098 kms^{-1}, which as expected is much smaller than the typical transverse velocity for halo stars, and therefore their effect on the proper motion difference in our catalogue should be negligible.

Therefore, measurement errors will be of much greater influence on the data in our catalogue. To put a limit on the proper-motion difference caused by these errors, a simple criterion was created that requires that the individual star-to-star proper-motion difference in both RA and DEC be no more than twice the stated error, which we interpret as a standard deviation. This criterion makes use of the individual errors available for each source, rather than being an absolute upper proper-motion difference limit.

Two standard deviations (with an average of $\sigma = 5.03$ mas yr^{-1}) was decided upon by trial and error while working with the data. This could be refined for individual binaries by obtaining accurate distance (both to Earth and the pairs' separation) and mass measurements (or reasonable estimates using isochrones) for individual pairs, which would allow more accurate orbital motions to be calculated. This could then be combined with the statistical errors to create an improved proper-motion difference limit for individual pairs.

3.4   Galactic Plane, LMC and SMC

Due to the focus of the project being on stars in the halo, disk and bulge stars are of no interest for our catalogue, therefore $\pm 15°$ around the galactic plane have been removed from the catalogue. This limit was chosen to hopefully remove the majority of unwanted disk stars while not removing too many legitimate halo stars.

The equation of the Galactic latitude is (Cox, 2000 citing Lang, 1980);

$$\sin(b) = \sin(\delta) \cos(62.87°) - \cos(\delta) \sin(\alpha - 282.86°) \sin(62.87°) \tag{3.5}$$

A secondary benefit of removing this region is that due to the density of stars in this region, spurious pairing becomes a much greater issue compared with those found further from the Galactic Plane.

The portion of sky containing the Large and Small Magellanic Clouds has also been removed, as we are only interested in halo stars in our own galaxy, and these dense regions contain many non-halo stars. A rectangle with the dimensions of;

$$0° < RA < 90° \text{ and} - 80° < Dec < -60°$$

was chosen to ensure the complete removal of sources from these two regions.

These exclusions are obvious in Fig. 3.4 which shows the dense regions of the Galactic Plane and the LMC and SMC and the removed sections surrounding them.
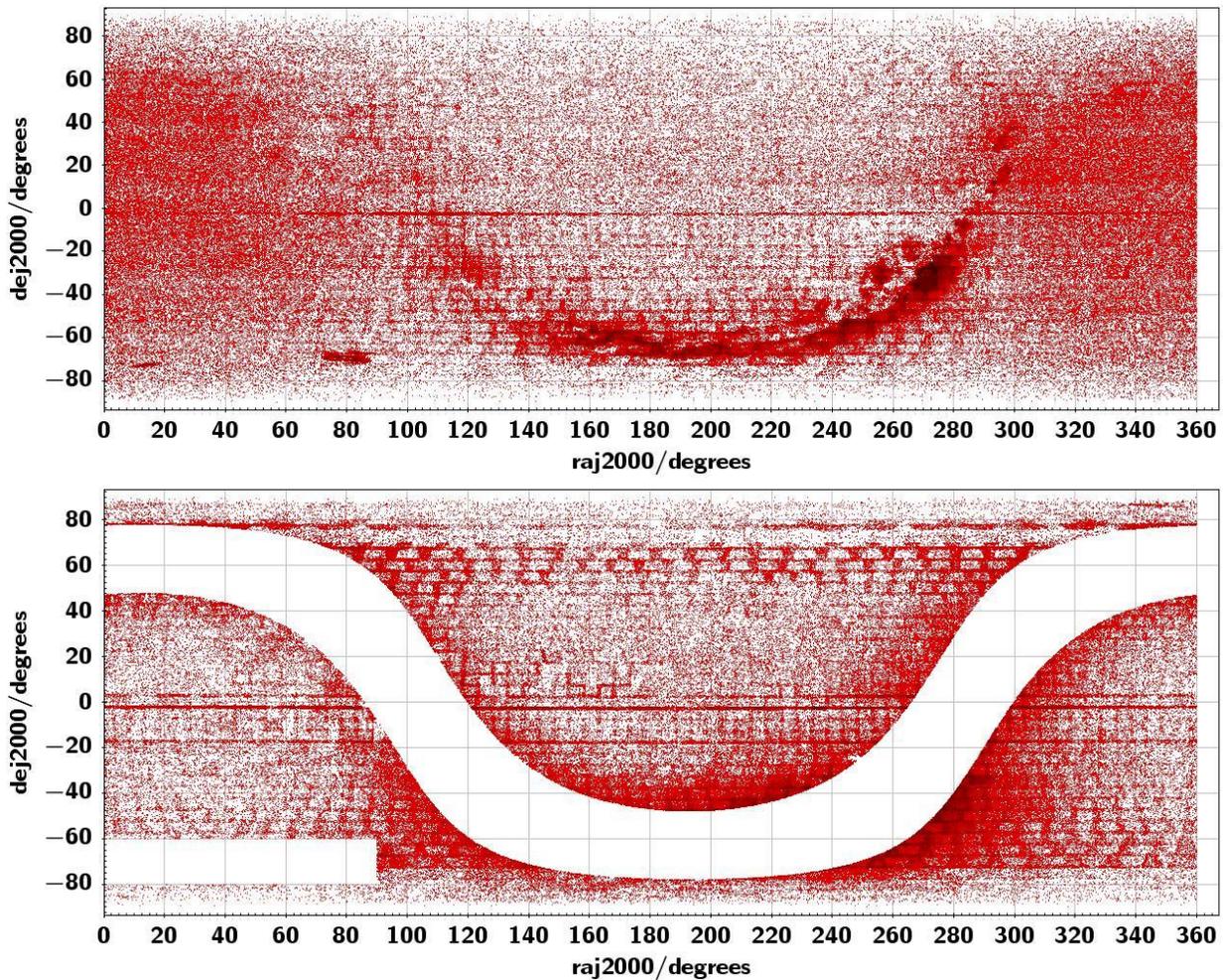
Figure 3.4   PPMXL data showing the areas to be removed using the above selection criteria, within 15° of the Galactic plane and near the LMC & SMC. The darker regions in the upper plot indicate a greatly increased density of stars (most of which are unwanted for the project. The brickwork pattern is discussed in Ch. 4.1).

Note: Due to technical problems with the TAPHandle service at the time of writing, the upper plot was created using randomly chosen criteria (pmra/e_pmra > 12 and b2mag < 15). The lower plot uses data from the final catalogue.

3.5   Angular Separation

Some work towards specifying the limits of the angular and physical separation of the stars was performed; however, problems arose with the catalogue before this criterion could be implemented, but the preparatory work has been included here.

A step in determining a pair's legitimacy is to identify whether a pair of stars with common proper-motions are physically close enough to be a binary system. This can easily be done by calculating the physical separation between the two sources and excluding any above a specific value. To determine this value, I compared two works. The first (Chanamé & Gould (2004), their Figure 10) covers a search for wide disk and halo binaries. As part of their analysis they give the physical separation distribution of binaries which should hold for the PPMXL catalogue. The second, (Lépine (2011), their Figure 2) also concerns wide binary systems but includes a comparison of the angular separation of binaries in the LSPM catalogue with those expected to appear due to chance alignments, shown in Figure 3.5. This comes from the number density of stars in a given area of sky, which are given by $n_* = \frac{dN}{dA}$. If we search an annulus of radius r and width dr around a star, the annular area is given as $dA = 2\pi r \, dr$, so we get $\frac{dN}{dr} = 2\pi r n_*$. Thus, the number of chance pairings will scale linearly with separation r. This holds whether r is expressed as an angular measure, e.g. in arcsec, or physical separation, e.g. in AU. As PPMXL and LSPM have been constructed in similar manners (scanning photographic plates, e.g. POSS I and POSS II) with both publishing all sources identified (rather than imposing a specific criteria such as high-proper-motion like the NLTT catalogue) and both having similar sensitivities and limiting magnitudes, the assumption has been made that Lépine's comparison using LSPM would also hold for PPMXL.
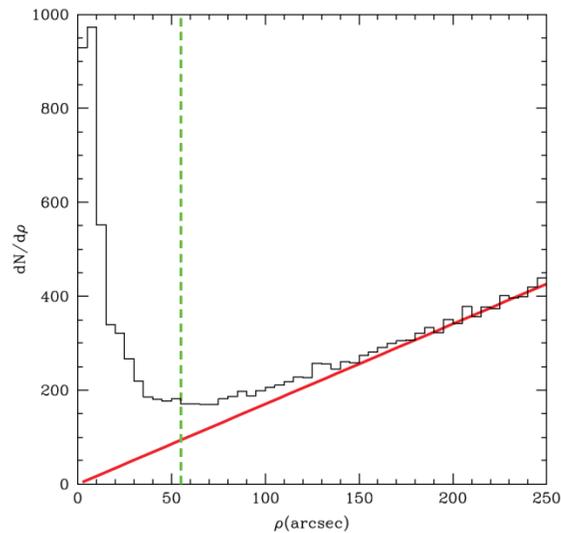
Figure 3.5:   Number of pairings as a function of their angular separation. The continuous line shows what is expected for chance alignments, the dashed line shows the separation (arcsec) at which 50% of sources are physical pairs. Taken from Lépine (2011), Figure 2.

From Lépine's comparison, the real pair detection percentage can be found as a function of angular separation (e.g. from Fig. 3.5, at 40" separation, 60% of detected pairs will be real binaries). Converting these angular separations to physical separations (using Chanamé's distance of 240pc) and applying these to the physical separation distribution of binaries gives the percentage of real binaries lost by imposing various physical separation limits (e.g. by imposing a maximum separation of $10^3 \, AU$, 61% of real binaries will be lost).

I decided that for the present investigation, a 10% real pair detection rate (where 10% of stars found are real, with 90% being false pairings) would be an acceptable compromise between gaining real pairs and the extra work to observe and subsequently remove the increased number of chance pairings while losing a small number of real binaries.

This corresponds to an outer physical separation limit of $10^{4.4} \, AU$, which removes ~22% of real binaries that exist at greater separations. This would need to be converted into an angular separation to be used as a criteria for the catalogue and would require the star's distance to be calculated which can be done using the star's photometry.

At present, my query searches out to 0.1° (6 arcmin) for companions (5th line in Fig 3.7), which according to Lepiné's work is likely to include a very large number of false pairings. Despite this,

it was decided to include this large criterion, in the hope of including all possible pairings in our initial searches, and using the work discussed Ch. 3.6 to refine the data at a later time.

Chanamé uses a value of 240 pc in his calculations; and though it was found that the average distance in the final catalogue was around 500 pc, it was decided that as we were trying to be as inclusive as possible with our radius of 0.1°, we will be obtaining many false pairings anyway, and so the work here is used as a guide for what detection rates are likely to be in our own catalogue.

3.6   Final Query

The above sections cover explanations for the use of the different selection criteria, and the final values used for the creation of the final catalogue; but they do not show how these criteria are implemented on the catalogue. There are also several smaller steps that were used in the query to improve the quality of the resulting catalogue, which are not mentioned above. The final query is included here (Fig. 3.7), with short explanations on the following pages as to what each line is doing to the catalogue.

```
SELECT TOP 1000000000 *

FROM ppmxl.main as ppmxl

left outer join ppmxl.main as ppmxli

on 1=CONTAINS(POINT('', ppmxl.raj2000, ppmxl.dej2000),

CIRCLE('', ppmxli.raj2000, ppmxli.dej2000, 0.1))

Where abs(ppmxl.ipix-ppmxli.ipix)>0

and ((abs((ppmxl.pmra-
ppmxli.pmra)/(power(ppmxl.e_pmra*ppmxl.e_pmra+ppmxli.e_pmra*ppmxli.e_pmra, 0.5)))<2)

and (abs((ppmxl.pmde-
ppmxli.pmde)/(power(ppmxl.e_pmde*ppmxl.e_pmde+ppmxli.e_pmde*ppmxli.e_pmde, 0.5)))<2))

and (abs(ppmxl.raj2000-ppmxli.raj2000)*cos(radians(ppmxl.dej2000))>0.0005 or abs(ppmxl.dej2000-
ppmxli.dej2000)>0.0005)

and ppmxl.jmag>=ppmxli.jmag

and (ppmxl.jmag-ppmxl.kmag)-(ppmxli.jmag-ppmxli.kmag)>0

and ppmxl.jmag-ppmxl.kmag>0.15 and ppmxl.jmag-ppmxl.kmag<0.65

and (abs(ppmxl.pmra/ppmxl.e_pmra)>5 or abs(ppmxl.pmde/ppmxl.e_pmde)>5)

and
ppmxl.jmag+5*log10(0.0000001+3600*power(ppmxl.pmra*ppmxl.pmra+ppmxl.pmde*ppmxl.pmde,0.5))
+5>9.6*(ppmxl.jmag-ppmxl.kmag)+9

and ppmxli.jmag-ppmxli.kmag>0.15 and ppmxli.jmag-ppmxli.kmag<0.65

and (abs(ppmxli.pmra/ppmxli.e_pmra)>5 or abs(ppmxli.pmde/ppmxli.e_pmde)>5)

and
ppmxli.jmag+5*log10(0.0000001+3600*power(ppmxli.pmra*ppmxli.pmra+ppmxli.pmde*ppmxli.pmde,0.
5))+5>9.6*(ppmxli.jmag-ppmxli.kmag)+9

and abs(sin(radians(ppmxl.dej2000))*cos(radians(62.87))-
cos(radians(ppmxl.dej2000))*sin(radians(ppmxl.raj2000-282.86))*sin(radians(62.87)))>0.2588

and (ppmxl.raj2000>90 or (ppmxl.dej2000>-60 or ppmxl.dej2000<-80))

and (power(ppmxl.pmra*ppmxl.pmra+ppmxl.pmde*ppmxl.pmde,0.5)>0.0000278)

and ((ppmxl.pmra>0.0001 or ppmxl.pmra<0.00005) or (ppmxl.pmde<-0.00002 or ppmxl.pmde>0.00002))
```

Figure 3.7   The finished version of the query imposed on PPMXL, which was used to create
our catalogue.

The steps that the query in Figure 3.7 goes through when imposed on the PPMXL catalogue are;

1. (SELECT TOP 1000000000 *) was used as a method to ensure all possible sources in the catalogue were included. As the full catalogue only includes ~900 million sources, requesting 1 billion results will return every possible result (which is potentially $(900\text{x}10^6)^2$ pairs). During testing, this number was lowered to produce much smaller samples of data.

2. The next 4 lines are a feature in TAPHANDLE which allows the catalogue to be paired with itself (catalogue 1 being named ppmxl and catalogue 2 being named ppmxli) based on sources in catalogue 2 within a radius of 0.1 degrees of the position of each source in catalogue 1. This is used to create a shorter list of candidates on which to impose the stricter selection criteria.

3. As the above step pairs sources based on a radius from a position, duplicate sources are included where the source is paired with itself in the second catalogue. (abs(ppmxl.ipix-ppmxli.ipix)>0) is used to remove these duplicates. Ppmxl.ipix refers to the variable ipix in the ppmxl catalogue, which is the catalogue ID number for each source. For a star that pairs with itself, these numbers will be the same. The function 'abs(x)' calculates the absolute value of x.

4. The next two lines remove any sources which do not meet the proper-motion difference criteria covered in Ch. 3.3 in both RA and DEC. The function 'power$(a*a + b*b, 0.5)$' evaluates $(a^2 + b^2)^{\frac{1}{2}}$, which is used to calculate the sum of errors added in quadrature.

5. Removal of pairs with separations below 0.0005°, as pairs below this limit tended to be duplicates of the star. This problem is covered in more detail in Ch. 4. The positions and proper motions in PPMXL are given in degrees, whereas the TAPHANDLE trigonometric functions expect arguments in radians, so the function 'radians(x)' is used to convert an angle in degrees into radians.

6. By ensuring that the J magnitude of star 1 is greater than or equal to that of star 2, we remove the majority of repeat pairings. Without this line, star A with star B and star B with star A are both included in the catalogue. Rare cases where $J_A = J_B$ are, for the present, retained as duplicates.

7. J-K colour cuts that force star 1 to be redder than star 2, as combined with the previous line, will select pairs where star 1 is fainter and redder than star 2, and thus likely to be a pair of main-sequence stars, i.e. are more likely to produce the sources we are interested in.

8. J-K colour cuts are imposed on star 1 (see Figure 3.3).

9. The high significant proper-motion requirement in at least one direction is imposed on star 1.

10. RPM cut is imposed on star 1 (see Figure 3.3). A small addition to the proper motion of $0.0000001 \, \mathrm{arcsec \, yr^{-1}}$ was necessary to prevent the TAPHANDLE query crashing in cases where the proper motion of the source was zero and was passed as an invalid argument to the function $\log 10(x)$.

11. The criteria from steps 7-10 are then imposed on star 2.

12. The removal of the Galactic plane (see Eq. 3.3), LMC and SMC.

13. Removal of a small region at the centre of the proper motion distribution, removing sources with lower proper motions.

14. Removal of a small portion of the proper-motion distribution, which we believe to be anomalous, as is discussed in Ch. 4.2.

4.0　Analysis and Interpretation

By imposing the selection criteria of Fig. 3.7 on the PPMXL catalogue, we obtain roughly 17,500 candidate halo CPM pairs, each with 2MASS photometry. Each of these pairs should have significant proper-motions, be found within a region of the RPM diagram that makes them likely to be main-sequence halo stars and have similar proper-motions to each other.

The following analyses have been performed to ascertain the quality and reliability of the content of this new catalogue of candidates. As will become apparent, the catalogue did not live up to the expectations and exhibited a significant number of problems.

4.1　Plate Boundaries

It was found when plotting RA vs Dec for the catalogue that a brickwork pattern is very prominent. This can be seen in Fig 4.1.
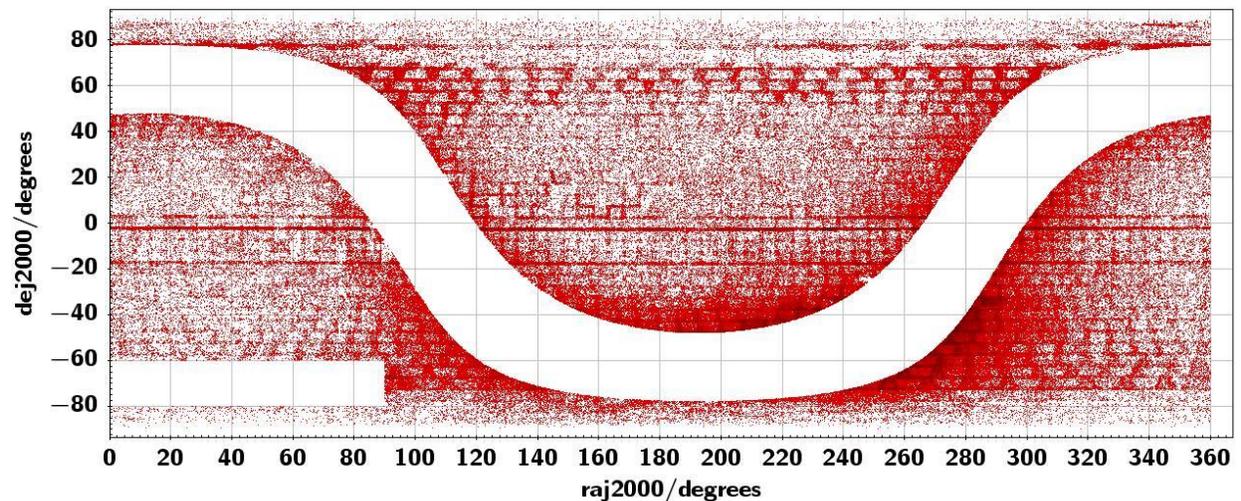
Figure 4.1: RA vs Dec for the halo candidate data, showing the brickwork pattern

The cause of these features is almost certainly associated with the plate boundaries from the photographic plates (see Ch. 2.1.4) which make up the original astrometric catalogue which was generated from scans of Schmidt plates. Two possible causes of the over-density are that when identifying stars in the regions where the photographic plates overlap, some sources are counted multiple times and/or the proper motions are not as accurate, causing much greater densities of either false stars or false proper motions in these areas, which creates the apparent brickwork pattern found in our catalogue.

While the source of this problem is known, no adequate solution was found without having to make a visual confirmation of each binary candidate, so this problem persists in the final catalogue, which means there is a portion of our catalogue consisting of spurious entries.

4.2   Proper-Motion Spike

The proper-motion distribution of the catalogue before the addition of the final line in the selection criteria shown in Fig 3.7 shows that there is an increased number of sources having positive proper motions in right ascension and almost zero proper motion in declination, which we refer to as the 'PM spike', highlighted in Figure 4.2. Though the distribution should be asymmetrical due to the reflex solar motion, this does not account for the increased density found in the PM spike feature shown below.
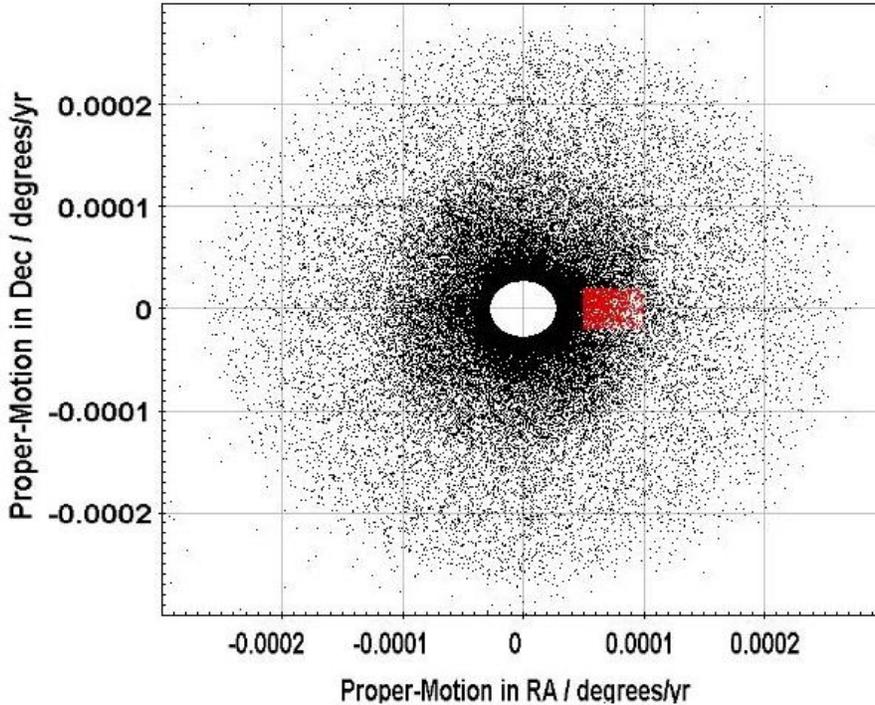
Figure 4.2: Proper-motion distribution for my catalogue with the pm spike criteria removed from the query, showing an increased density of sources in the positive x-axis.

Note: Due to changes in the catalogue search function over the course of this research, we are now unable to regenerate exactly the same subsample as that in which the PM spike was first identified without the search timing out.

However, from the data in the catalogue, no significant differences in position, magnitude or colour could be found between the sources in the PM spike and those elsewhere in the distribution. There are a large number of these sources found near the Galactic Plane and in the plate boundary features detailed above, however it is not known if these features are the cause, or if there are simply more sources found there because they are denser regions.

As no cause could be identified, it was decided that it would be best to remove the section of 0.5×10^{-4} °/yr^{-1} $< pmra < 1 \times 10^{-4}$ °/yr^{-1} and -2×10^{-5} °/yr^{-1} $< pmde < 2 \times 10^{-5}$ °/yr^{-1} from the catalogue, to improve the overall quality.

4.3   Colour and Magnitude Differences

Although colour and magnitude selection criteria were imposed (Fig. 3.7) that should have produced pairs where the first star is fainter and redder than the second, consistent with them lying on the halo main sequence (Fig. 3.3), it was noticed during the early parts of analysing the catalogue that there was a lack of any sort of correlation between the colour difference $(J-K)_1 - (J-K)_2$ and the magnitude difference $J_1 - J_2$ that would have suggested that the catalogue was composed primarily of main-sequence, CPM halo stars.

To test this lack of correlation, I decided to make use of the Padova isochrones used previously. Using the data for low metallicity ($Z = 0.0001$), typical halo age ($\log(age\,/\,\mathrm{yr}) = 10.05$) for a range of initial masses between $0.15M_\odot$ and $0.8492M_\odot$ (the mass range provided by Padova that corresponds to the main-sequence colour range $J-K < 0.65$), theoretical binaries were created by pairing each computed magnitude and colour in the isochrone with every other computed magnitude and colour, to form a simulated set of theoretical binary pairs (Fig. 4.3).
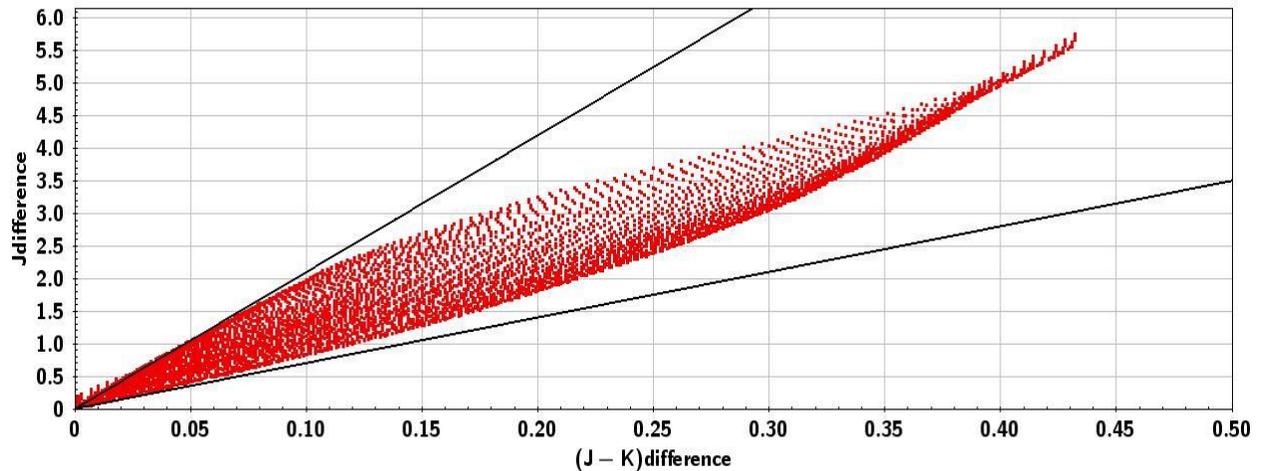
Figure 4.3   Theoretical binaries from Padova isochrones in the region constrained by limits from Fig. 3.7, for pairings between two main sequence stars.

Figure 4.3 shows a plot of ΔJ vs $\Delta(J - K)$, where $\Delta J = J_{star\ 1} - J_{star\ 2}$ and $\Delta(J - K) = (J_{star\ 1} - K_{star\ 1}) - (J_{star\ 2} - K_{star\ 2})$ for the theoretical isochrones; the black lines in the figure enclose the region where the two stars of the theoretical pair are both located on the main sequence. Stars located above this region are pairings between main-sequence/sub-giant and sub-giant/sub-giant are found, as these pairings have a greater difference in J for a given J-K difference than those found on the main sequence. In theory, when comparing the catalogue pairs with these theoretical pairings, high density regions should be found corresponding to the different combinations of binaries.

Making the same plot using the data from my catalogue, as shown in Fig. 4.4, it is plain that none of the features found in Fig. 4.3 are evident in our data. As our search criteria were based on main-sequence pairings, there should have been at least some correlation found in the region enclosed by the black lines.

This lack of any correlation in the observed data would suggest two possible causes; either that the catalogue contains a large number of chance (unphysical) pairings, or that fictitious data (fictitious sources and/or unrealistic proper motion values) have compromised the catalogue.

A third possible problem could be that theoretical binaries created using the Padova isochrones are not an accurate representation of the real CPM halo binaries in the PPMXL catalogue, but due to the fact no features at all are present in the catalogue's data (Fig. 4.4), even if the theoretical binaries are incorrect, there is still a major problem with our catalogue, likely because of one of the reasons mentioned above.

For reference, data for the stars in a known CPM binary list (discussed in Ch. 4.4) has been included in Fig 4.4 as indicated by the blue diamonds.

It should also be noted that the black lines in Fig. 4.4 do not allow for photometric uncertainty and requires perfectly identical colour/magnitudes for same type pairs. This is considered further in Ch. 4.5.
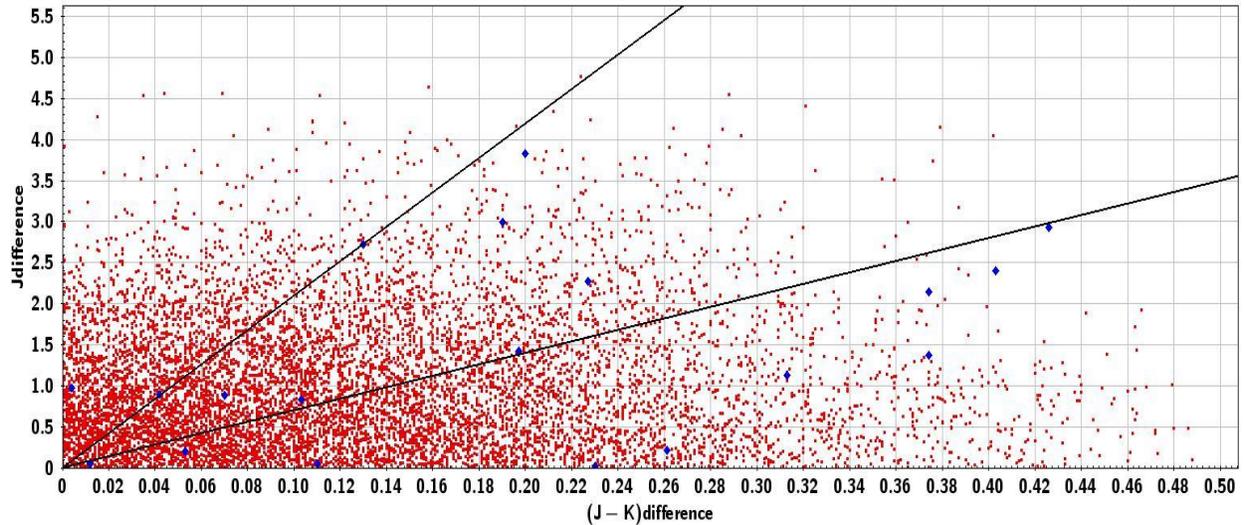
Figure 4.4   Data for our catalogue for the same region found in Fig. 4.3, showing little correlation, or features that were expected. Blue diamonds indicate data from a known CPM binary list discussed in Ch. 4.4.

4.4   Known List Comparison

To determine whether the lack of correlation is caused by erroneous data, or if false pairings with irrelevant sources like disk stars are obscuring the halo stars, we decided to use some previously studied CPM binaries and attempt to identify them in our data.

4.4.1 Known CPM Binary List

A small list of 25 CPM pairs compiled by Ryan (1992) was used for the comparison. These stars are sourced from the original NLTT catalogue based on several constraints similar to the ones which have been imposed on our own catalogue, with a focus on halo common-proper-motion pairs, with some metal poor examples noted in the list.

As these pairs have been identified in an older catalogue than that which we used for the project, it is hoped that the increased sensitivity of the PPMXL data means if these stars are present in our catalogue, they should be easily identifiable.

4.4.2   Cross-Matching With Our Catalogue

The method chosen for cross-matching the list with our catalogue used improved and updated coordinates for the NLTT stars from SIMBAD[3]. SIMBAD data are gathered from a range of catalogues, such as Hipparcos and Tycho-2. The exact data source used varies for each star. I conducted a search for any sources within a radius of up to 0.3 degrees of each star's coordinates in our catalogue. The proper-motions and photographic magnitudes were then used to identify the correct star where possible.

Using this method, only 35 of the 50 stars on the list, making 13 complete pairs and 9 individuals, were identified in our ~17,500 pair catalogue. Of the 15 stars not identified in our catalogue, 11 met the selection criteria including CPM cuts and should therefore have been present in the final catalogue. This is a mixed result, as it would suggest that the catalogue contains at least some halo CPM pairs.

It was noticed during the cross-matching process that some of the NLTT CPM sources, have wildly different proper-motion values for the two stars comprising the supposed pair, to the extent that some sources appear to be travelling in the opposite direction to what they were expected to as suggested by both the known CPM list and the data found on SIMBAD.

---

[3] **http://cds.u-strasbg.fr/**

4.4.3 Comparing Sources of Data

To attempt to find the cause of the differences between the data from PPMXL and that of the Ryan (1992) CPM list, a comparison of the proper-motions for PPMXL, USNO-B1, NLTT, rNLTT and various sources taken from SIMBAD was made, as shown in Table 4.1.

For roughly half of the list, the proper-motions of the sources are largely different from those provided by rNLTT and the SIMBAD sources, with a large number of these differences also occurring in the USNO-B1 catalogue.

It was initially thought that there must be an error in how the PPMXL catalogue was created due to the inconsistencies noted during the cross-matching with the previous CPM list. However, from the table; it can be seen that for the majority of the sources which have these large proper-motion differences compared with outside sources, USNO-B1 sources also provide data with similar large differences with the outside sources. This would suggest that USNO-B1 is more likely the cause of the problems we've encountered in PPMXL, since PPMXL is based on USNO-B1; and errors that were created in the USNO-B1 catalogue will have persisted through the newer catalogue, and into ours.

It was noted in the caveats for USNO-B1, Ch. 2.1.4, that during its creation, any movement for a source that could be attributed to motion in a straight line was included in the catalogue, which has caused a large number of non-existent sources and sources with incorrect proper-motions to be written into the catalogue. It is possible that this is the cause in the large variations in proper-motions between the different source catalogues.

Pair number	Name	Our catalogue				PPMXL				rNLTT				NLTT				USNO-B1				Hipparcos				Tycho-2				Liv-Ed				LSPM				Remarks	Field image problems
		pmra	e_pmra	pmdec	e_pmdec	pmra	e_pmra	pmdec	e_pmdec	pmra	e_pmra	pmdec	e_pmdec	pmra	e_pmra	pmdec	e_pmdec	pmra	e_pmra	pmdec	e_pmdec	pmra	e_pmra	pmdec	e_pmdec	pmra	e_pmra	pmdec	e_pmdec	pmra	e_pmra	pmdec	e_pmdec	pmra	e_pmra	pmdec	e_pmdec		
1	LHS 1281	328.97	2.9	-450.8	3.1	329.0	2.9	-450.8	3.1	319.9	1.8	-435.8	1.8	316.2		-474.3		318		-454		321.44		-452.69														USNO-B1 records large difference in PM between the pair	crosshair and multiple
	LHS 1279									319.9	1.8	-435.8	1.8	316.2		-474.3		104	19	-406																			
2	L91-93	176.29	2.1	-1.8	2.1	176.3	2.1	-1.8	2.1	176.9	2.1	-1.8	2.1	199.0		-12.5		176	19	-2		176.3	2.1	-1.8	2.1													Large difference in pmRA between the pair	multiple sources
	L91-94	131.21	34.2	233.3	34.2	131.2	34.2	233.3	34.2	176.3	2.1	-1.8	2.0	199.0		-12.5																							
3	LP230-119	168.1	8.7	-199.2	8.7	168.1	8.7	-199.2	8.7									194.0	30	-260.0	32									190		-210							faint crosshairs
	LP230-125																																							
4	LP201-31													94.5		-110		30.0	39	-182.0	19																	Binarity flag in rNLTT but not present in list; does not match Simbad data	
	LP201-30					90.3	10.9	-141.6	9.3	94.0	20	-110.0	20																										
5	G99-8	254.56	3.9	49.16	3.9	254.6	3.9	49.2	3.9									264.0	2	46.0	3													258.0		57.0			
	G99-9	255.53	3.9	51.95	3.9	255.6	3.9	52.0	3.9									256.0	2	54.0	4													258.0		57.0			
6	LP839-39	-257.64	7	-83.3	7	-257.6	7	-83.3	7	-176.6	5.5	-154.9	5.5	-215.3		-108.3		-258.0	4	-82.0	15																	Large difference between USNO-B and ; 0 errors?	multiple sources
	LP830-38									-176.4	0	-154.9	0	-215.3		-108.3																							
7	G192-57	80.07	4	-282.36	4	80.1	4	-282.4	4									82.0	3	-278.0	1													86.0		-280.0		Large difference between the two sources	
	LP122-11	-51.71	4	-232.08	4	-51.7	4	-232.0	4									-46.0	2	-226.0	4													-47.0		-231.0			
8	G112-43	-169.6	1.4	-305.6	1.4	-169.6	1.4	-305.6	1.4	-169.6	1.4	-305.6	1.4	-113.6		-277.7		-170.0	9	-306.0		-192.58		-298.48														Wildly different PM values in PPMXL relative to other sources	
	G112-44	-102.61	17.7	96.19	17.4	-102.6	17.7	96.2	17.4	-175.1	19.4	-294.8	11.7	-113.6		-277.7		-176.0	20	-236.0		-165.78		-307.48															
9	G113-9	87.67	1.5	-303.91	1.5	87.7	1.6	-303.9	1.5	85.6	0	-302.3	0	89.4		-279.0		84.0	9	-304.0						85.6		-302.3										0 errors?	
	LP664-40									85.6	0	-302.3	0	89.4		-279.0																						No options in USNO-B with similar magnitudes	
10	G251-54	136.53	0.9	-366.46	0.9	136.5	0.9	-366.5	0.9	135.0	1.8	-365.1	1.8	159.6		-364.6		134.0	9	-366.0		135.5		-366.26															faint crosshair
	G251-53	131.07	3.9	-366.08	3.9	131.1	3.9	-366.1	3.9	132.4	5.5	-360.6	5.5	159.6		-364.6		136.0	1	-364.0	3	138.0		-376															
11	LP791-8	-200.5	2.3	-170.91	2.3	-200.5	2.3	-170.9	2.3	-202.4	2.4	-169.4	2.6	-219.2		-116.1		-204.0	11	-170.0		-195.23		-164.5														Not found in PPMXL or USNO-B	faint crosshair
	LP791-7									-197.6	5.5	-159.3	5.5	-219.2		-116.1																							
12	LP850-24	-312.96	2.4	55.3	2.5	-313.0	2.4	55.3	2.5	-320.0	3.2	63.1	3	-310.1		60.6		-320.0		62.0						-320.0		63.1											crosshair from field star
	LP850-23	-314.11	4.1	58.44	4.1	-314.1	4.1	58.4	4.1	-301.9	5.5	65.6	5.5	-310.1		60.6		-312.0		58.0																			

#	Source	Col 1 (pmRA, pmDE)	Col 2 (pmRA, pmDE)	Col 3 (pmRA, pmDE)	Col 4 (pmRA, pmDE)	Col 5 (pmRA, pmDE)	Col 6 (pmRA, pmDE)	Col 7 (pmRA, pmDE)	Notes
13	1139+396			−134.6/6.5, −197.1/5.6	−163.6, −147.1			−183, −127	Large difference in pmde
	LP215-35	−195.11/3.3, −118.74/3.3	−195.1/3.3, −118.7/3.3	−183.1/3.5, −122.8/5.5	−163.6, −147.1				
14	LP265-582	−137.33/2.0, −63.99/2.0	−137.3/2.0, −64.0/2.0	−131.1/3.5, −73.7/3.3	−161.6, −126.2	−132.0/5, −74.0	−126.96, −64.76*		
	LP265-581		−137.3/2.0, −64.0/2.0	−131.1/3.5, −73.7/3.3	−161.6, −126.2	−134.0/5, −64.0	−126.96, −64.76*		
15	G63-5	−523.0/1.0, 269.14/1.0	−523.0/1.0, 269.1/1.0	−521.5/1.1, 269.4/1.1	−518.1, 263.0	−522.0/1, 268.0	−520.03, 267.36	−517, 269	crosshair
	G63-6	−524.6/4.8, 269.25/4.8	−524.6/4.8, 269.3/4.8		−518.1, 263.0	−516.0/5, 274.0/3			
16	G66-15	−291.25/1.2, 55.05/1.2	−291.3/1.2, 55.1/1.2	−288.3/1.2, 56.1/1.2	−271.9, 66.9	−290.0/1, 56	−285.92, 58.18		faint crosshair
	G66-16	−287.75/1.8, 64.31/1.8	−287.8/1.8, 64.3/1.8	−286.4/1.9, 68.3/1.8	−271.9, 66.9	−288.0/1, 68.0	−237.53, 64.70		
17	LHS53	−999.4/1.6, −3541.9/1.6	−999.4/1.6, −3541.9/1.6	−999.4/1.6, −3541.9/1.6	−1001.5, −3542.1	−1000.0/12, −3542.0	−997.47, −3543.55		
	LHS52	−1003.5/1.8, −3543.3/1.8	−1003.5/1.8, −3543.3/1.8	−998.9/1.5, −3544.6/1.5	−1001.5, −3542.2	−1000.0/12, −3546.0	−999.75, −3542.60		
18	LP745-22	−163.89/2.2, 145.43/2.2	−163.9/2.2, 145.4/2.2	−165.2/2.6, 144.4/2.9	−182.7, 136.4	−166.0/11, 144.0	−165.2, 144.4*		
	LP745-23	−167.4/2.2, 147.2/2.2	−167.4/2.2, 147.2/2.2	−166.7/3.7, 144.0/3.7	−182.7, 136.4	−166.0/4, 146.0/3	−166, 144*		
19	G262-21							219, 210	
	G262-22	216.77/12.5, 203.03/12.5	216.8/12.5, 203.0/12.5					219, 210	
20	LP636-3	−33.43/3.8, −180.82/3.8	−33.4/3.8, −180.8/3.8	−38.3/5.5, −186.1/5.5	−51.2, −180.9	−26.0/2, −178.0/3			multiple sources / Large difference in pmra
	LP636-2	−42.18/9.2, −182.76/9.2	−42.2/9.2, −182.8/9.4	−37.0/5.5, −185.4/5.5	−51.2, −180.9	−26/2, −178.0/3			
21	LP929-12	−80.26/3.4, −243.04/3.4	−80.3/3.4, −243.0/3.6	−86.8/5.5, −246.6/5.5	−88.7, −233.7	−86.0/1, −244.0/5			
	LP929-11	−80.13/4.0, −243.95/4.0	−80.1/4.0, −244.0/4.0	−88.3/5.5, −246.6/5.5	−88.7, −233.7	−88.0, −244.0/5			
22	LP82-11								
	LP82-12								
23	LP521-3	134.79/1.8, −99.11/1.8	135.0/1.9, 37.1/1.9	135.7/2, 36.6/2	134.0/2, 36.0	178.4, 65.3	135.7/2.0, 36.6/2.0	136, 37	multiple sources / Large difference between rNLTT and other sources
	LP521-4			134.6/5.5, 37.1/5.5		178.4, 65.3			
24	LP246-71	134.8/1.8, −99.1/1.8	134.8/1.8, −99.1/1.8	234.9/0, −152.5/0	23.2, −163.8	136.0/4, −100	87.33, −52.78	240, −153	Large differences between all source catalogues
	G74-47	235.6/4.2, −153.6/4.2	235.6/4.2, −153.6/4.2	234.9/5.5, −152.5/5.5	232.0, −163.8	234.0/3, −154.0/4			
25	LP520-70	112.11/1.8, −4.87/1.8	112.1/1.8, −4.9/1.8	109.3/1.9, −4.9/1.9	173.9, −4.63	108.0/2, −6.0	112.70, −4.8*	198, 6	Large difference between the two sources
	LP520-71	206.06/3.3, 151/3.3	206.1/3.3, 151/3.9			206.0/2, 6.0			

Table 4.1 (Notes)

Proper-Motions in the table are given in milli-arcsec per year (as opposed to deg/yr found in PPMXL).

Green shading indicates these sources suffered from the crosshair problem discussed in Ch. 4.4.4.

Yellow shading indicates these sources suffered from the multiple sources problem discussed in Ch. 4.4.4.

Some SIMBAD error ellipses were found to be untrustworthy (given semi-major axis was sometimes smaller than the semi-minor axis) and are replaced with '*'.

Where errors were not found (common with USNO-B1 sources), space has been left blank.

4.4.4 Field Comparisons

Due to the observed inconsistencies in proper-motion data between the catalogues, the fields around each source from USNO-B1, the Digital Sky Survey (DSS) and PPMXL were compared to attempt to identify any possible causes of the inconsistencies. These sources were all produced from the same plates, and therefore should contain almost all of the same sources as each other. A faintness limit of around $b \sim 22$ in the PPMXL plots is provided by requiring 2MASS data and is shown in Fig 3.2; though this should not affect the comparison too much as the sources are brighter than this limit.

Skrutskie et al. (their Figure 17, Skrutskie et al., 2006) shows that they could extract good photometry for stars as bright as $K_S = 4$. The brightest halo star is HD140283 which has $K = 5.6$ (SIMBAD[4]), so it is unlikely that any halo star has been rejected as a result of the bright limit of 2MASS.

Roeser et al. (their section 6.1, Roeser et al., 2010) claims that they are complete "from the brightest stars down to about 20th magnitude in V", so they probably have no bright limit either.

From these, two frequently recurring problems were identified, as detailed below.

1. The most common problem identified is evident in Figure 4.5, where there is a crosshair pattern of stars around the main source that do not exist in the DSS field, Figure 4.6. This is caused by oversaturation of the bright, main source in the centre being mistaken for multiple, non-existent stars and included in the final catalogue.
Not only does Fig 4.5 reveal a large number of fictitious stars in the field, it is also obvious that the relative position of the brightest central source in Fig. 4.5 and the brightest source in the SW quadrant does not match the relative positions seen in Fig 4.6. In short, it does not appear possible to derive even relative data for the two

---

[4] http://simbad.u-strasbg.fr/simbad/sim-basic?Ident=hd140283&submit=SIMBAD+search#lab_basic

components of LHS 1281/1279. The addition of proper motion data in Fig 4.7 does not aid in the interpretation of this field either.
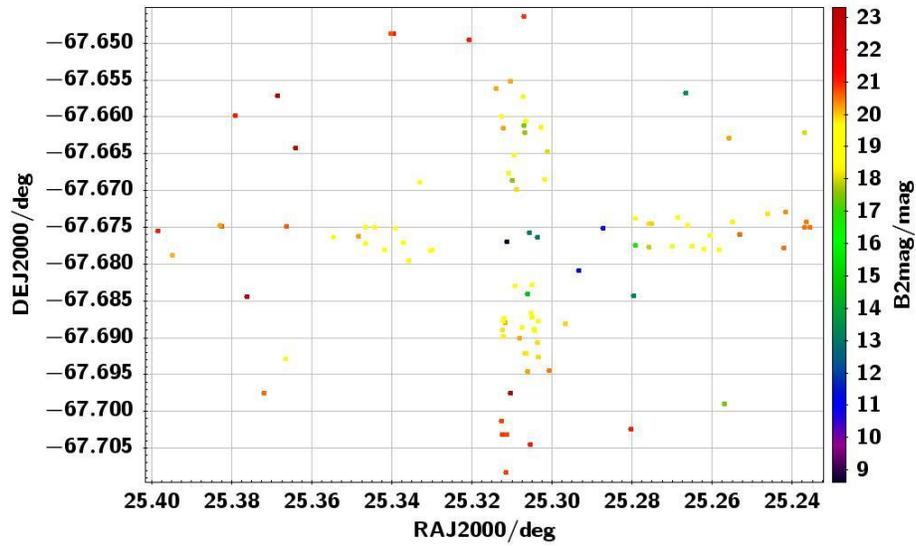
Figure 4.5   Plot of USNO-B1 sources within 2' radius of LHS 1281, showing the B2 magnitudes for each source. The plot contains 163 individual sources. The plot was created using TOPCAT.
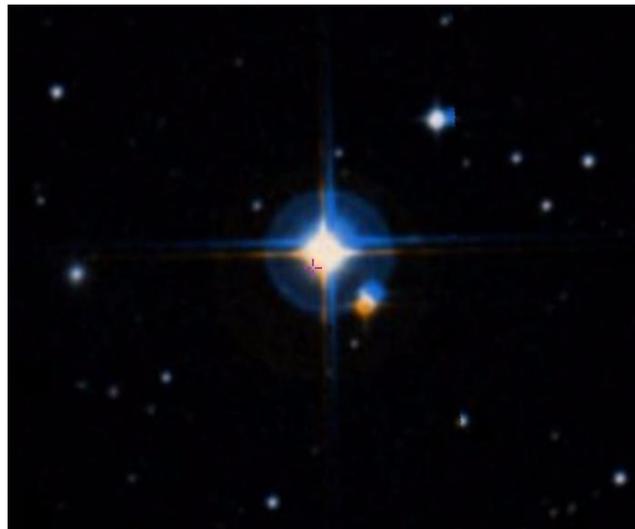
Figure 4.6   DSS image of LHS 1281. FOV: 7.19' From DSS2, likely using either the AAO-SES or SERC-I surveys[5]

---

[5] http://gsss.stsci.edu/SkySurveys/Surveys.htm
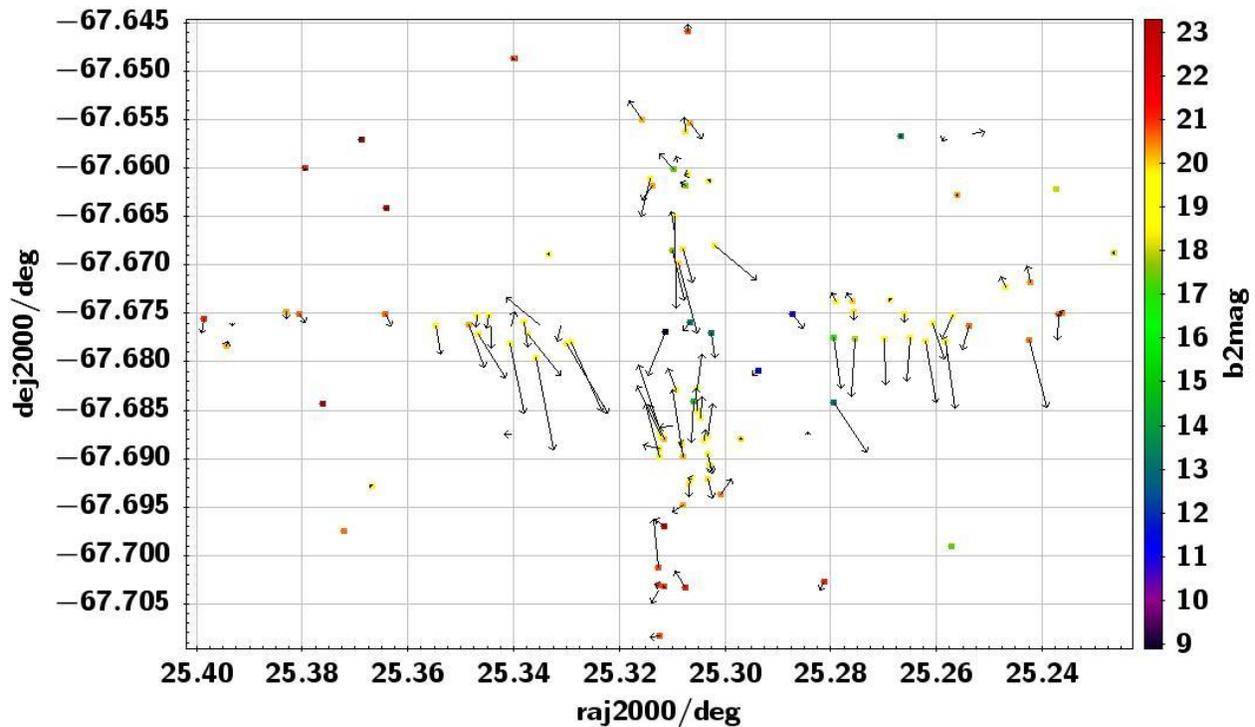
Figure 4.7   Plot of PPMXL sources within 2' of LHS 1281, showing the B2 magnitudes and proper motion vectors of each source. The plot contains 114 individual sources. Vector scale; 1mm : 80 mas/yr.

2. Another problem that was identified is where a bright source has been converted into multiple bright sources in its location, as shown in Figures 4.8 and 4.9, where the DSS image shows two bright stars in the centre of the field, but USNO-B1 records five such sources being present. The inclusion of proper motion vectors for the field (Fig. 4.10) shows a diverse series of measurements for these false stars, which are nevertheless larger than those of many objects in the field and hence can be misinterpreted as high proper motions. This is due to USNO-B1's decision to contain all possible matches and allow users to sort them for themselves; this problem has caused a large number of bright, false sources where they should only be one. Another problem caused by this decision is that as every possible match that could be attributed to motion in a straight line was included, many of these bright false stars have high proper-motions, which can cause problems when trying to identify the genuine source.
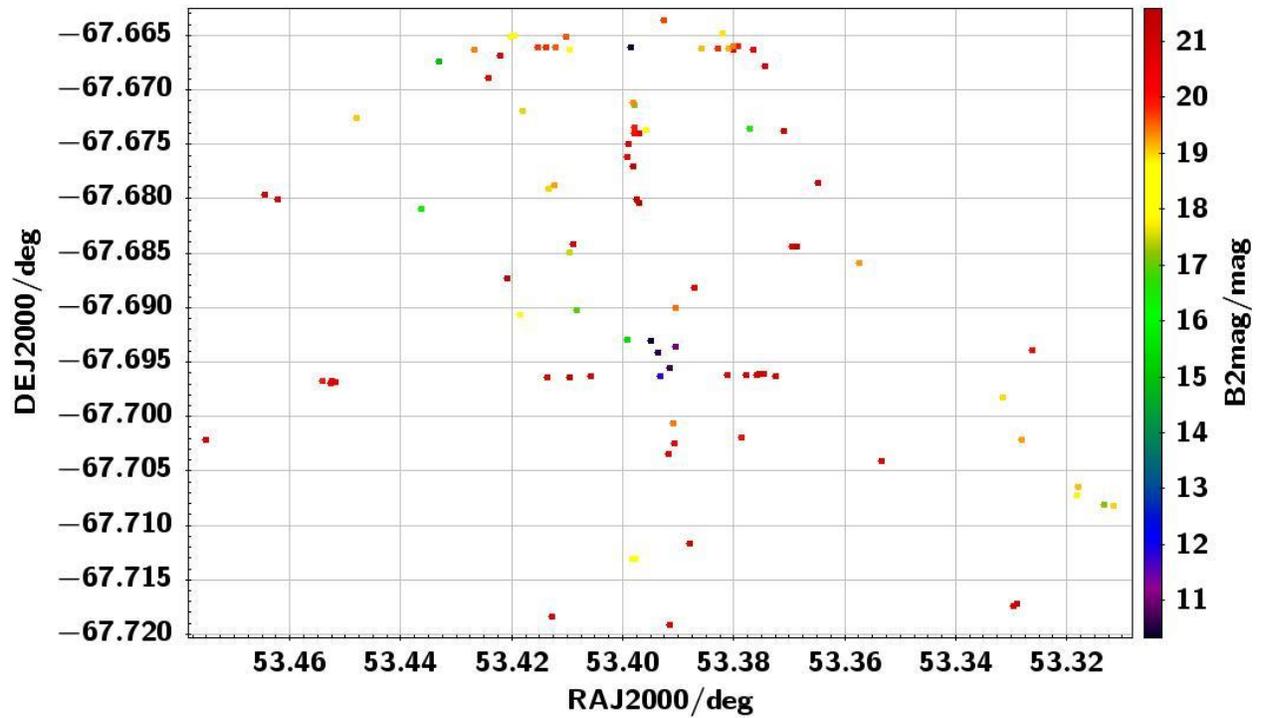
Figure 4.8   Plot of USNO-B1 sources within 2' of L91- 93, showing their B2 magnitudes. The plot includes 5 bright sources in the centre, where there should only be two.

Figure 4.9   DSS image of L91-93. FOV:8.08'.

From DSS2, likely using either the AAO-SES or SERC-I surveys[6]

[6] http://gsss.stsci.edu/SkySurveys/Surveys.htm
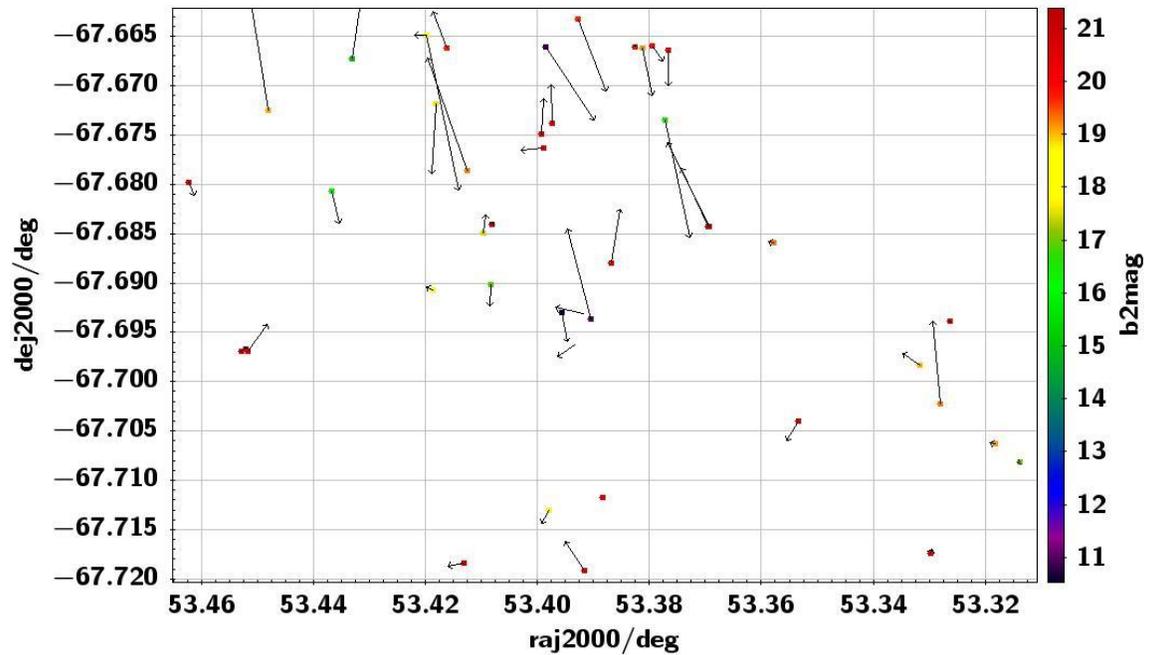
Figure 4.10   Plot of PPMXL sources within 2' of L91-93, showing their B2 magnitudes. Four of the five bright sources shown in Figure 4.8 are present. Vector scale; 1mm : 45 mas/yr.

Observing sources with a range of J magnitudes, it was found that the crosshair problem discussed above has a cut-off point of around $J > 11.5$. An example of a pair at roughly $J = 13$ is shown in Fig. 4.11, with its DSS counterpart shown in Fig. 4.12, where it is evident that diffraction spikes are no longer a problem.
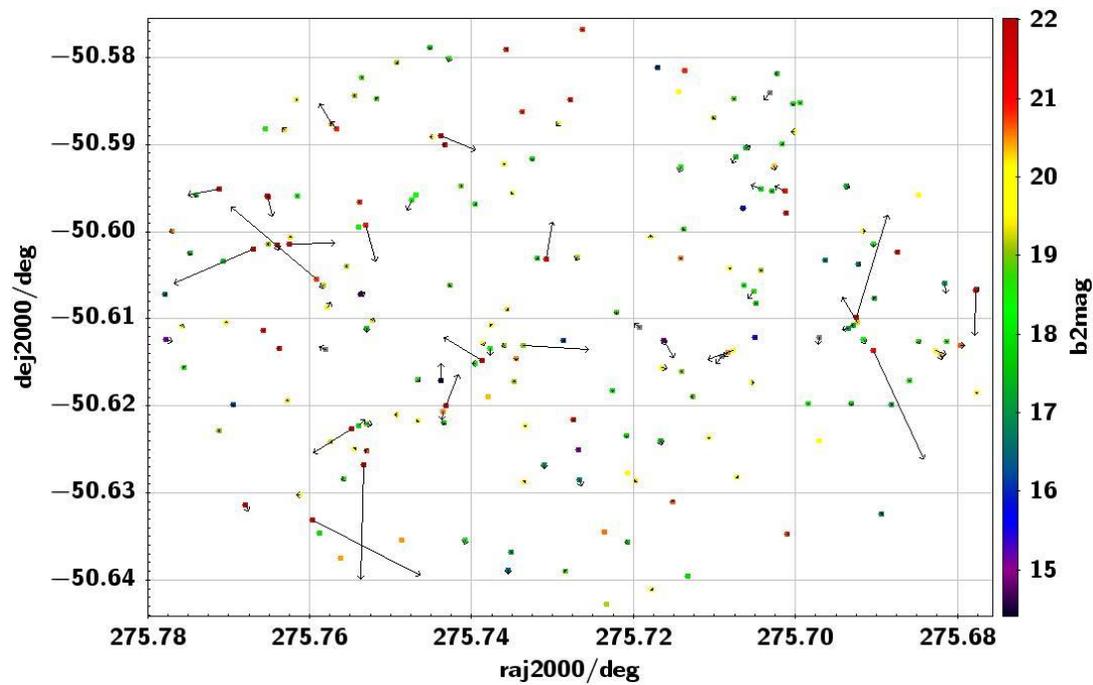
Figure 4.11   An example of a star from the final catalogue at J=13, at which point the crosshair problem has disappeared. Vector scale; 1mm : 55 mas/yr.
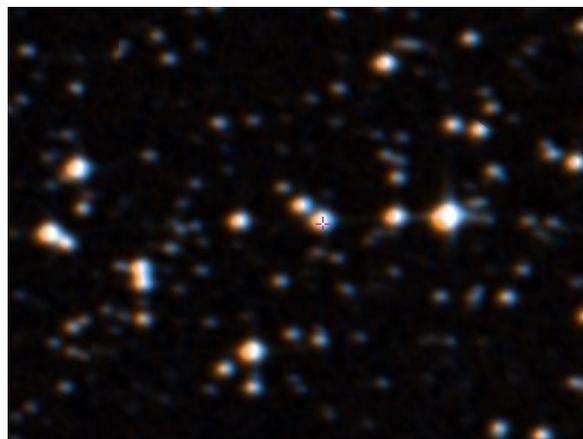
Figure 4.12   DSS plot corresponding to the region shown in Fig. 4.12. FOV: 7.2'.

From DSS2, likely using either the AAO-SES or SERC-I surveys[7]

---

[7] http://gsss.stsci.edu/SkySurveys/Surveys.htm

Additionally it was noted that for the majority of these sources with small J magnitudes, which is evident in Fig 4.11, USNO-B1 has a tendency to record two sources for the main stars where there should only be one. This error is possibly of some benefit, as it is possible that the multiple sources in these fields indicate that sources with proper-motions have been identified, with the different sources arising from plates from different epochs. These multiple sources could be used as a guide to identify more likely CPM candidates, by searching for sources in the USNO-B1 catalogue, and using the epochs available for the data to attempt to determine if sources from different epochs have linear motion that is consistent when ordered chronologically.

4.5   Final Catalogue Summary

Though we have shown that our final catalogue does contain a reasonable number of the previously suggested CPM halo binaries, we have also found that there are a large number of errors and inconsistencies in the USNO-B1 data when compared with those of multiple outside sources. Because of this, the data we have extracted from PPMXL, which uses USNO-B1, cannot be trusted for use in the future work we had planned for the project because there is a high chance that a randomly chosen source from our catalogue could be a disk star with incorrect proper-motion data, or that the source may not exist at all. This may be the cause behind the lack of correlation (ΔJ vs $\Delta J - K$) found between the catalogue data and the theoretical pairs shown in Figure 4.3; though whether this is the sole causes is not known for certain without further analysis.

The majority of the causes appear to be from the composition of the USNO-B1 catalogue, with its 'include every possibility' method of identifying sources, as this has added a large number of non-existent stars into the catalogue, many of which have large proper-motions, which means they are likely to be considered by our selection criteria as possible CPM main-sequence halo stars.

Based on the analysis presented in this chapter, further refinement of the selection criteria was undertaken. In order to select only those ΔJ and $\Delta J - K$ values compatible with the Padova isochrones (Fig. 4.3), we required that $7\Delta(J - K) < \Delta J < 21\Delta(J - K)$. To address the issue of the previous criteria not allowing for photometric uncertainty, a 3σ area around 0,0 has been included. To avoid problems associated with multiple 'crosshair' sources in the USNO-B1 catalogue arising from the diffraction spikes, a bright limit of $J = 11.5$ was to be set, however it was found that only 3 sources brighter than this limit were kept by the above criteria, and so it was not implemented.

Additional criteria suggested by Dr. Nigel Hambly and Prof. David Pinfield were also considered. Requiring at least one source in each pair to have a minimum of 3 observations helps to remove a large amount of the contamination found in the crosshair problem discusses in Ch. 4.4.4. Sources with only two observations are more likely to be a chance pairings than those with multiple observations.

Secondly the removal of sources with large χ^2 values as identified by PPMXL using the flags data can remove some spurious motions from the final catalogue. This value relates to the expected direction and speed of motion from observations and how much the measured values deviate from the expectations. Sources that differ greatly from the expected motion are more likely to be spurious.

These changes reduced the catalogue of ~17,500 pairs down to ~2,326 CPM pairs, which could in future be examined individually to verify which ones are worth observing to confirm their binarity.

The following criteria were added to the final selection criteria given in Fig. 3.7.

and (((ppmxl.jmag-ppmxli.jmag)-7*((ppmxl.jmag-ppmxl.kmag)-(ppmxli.jmag-ppmxli.kmag)))>0

and (ppmxl.jmag-ppmxli.jmag)-21*((ppmxl.jmag-ppmxl.kmag)-(ppmxli.jmag-ppmxli.kmag)))<0

or (ppmxl.jmag-ppmxli.jmag<0.2 and ppmxl.jmag-ppmxl.kmag-ppmxli.jmag-ppmxl.kmag<0.02))

and (ppmxl.nobs>2 or ppmxli.nobs>2)

and (ppmxl.flags !=1 or ppmxli.flags !=1)

Figure 4.13   Additional criteria created from the analysis to further refine the catalogue. Added onto the end of the criteria shown in Figure 3.7.

The significance of star 2's proper motion (its proper motion divided by its uncertainty, discussed in Ch. 3.1) was used to create a plot (Fig. 4.14) against the separations calculated in Ch. 3.3 to give some indications towards a likely candidate list
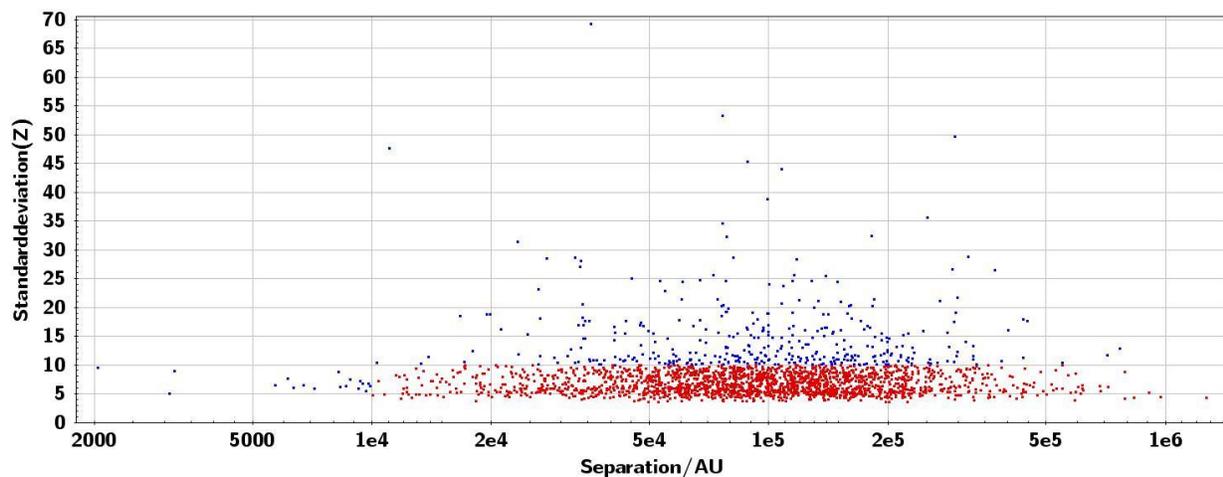
Figure 4.14   Significance of the proper motion of star 2 (number of standard deviations) vs the physical separation (AU) of the pair. Candidates with $Z > 10$ or Sep $< 1 \times 10^4$ AU have been highlighted in blue.

The highlighted data in Fig. 4.14 indicate the 318 pairs of sources we believe have an improved chance of being genuine pairs due to either their close separations or the significance of their proper-motions compared to their errors, and as such would be preferential candidates for potential follow-up observations.

The final catalogue of 2326 pairs of sources is located here:

http://star.herts.ac.uk/~sgryan/private/JohnSharkeyMSc/

The catalogue headings, units and descriptions are included here in Fig. 4.15. (_1 and _2 denote data relating to star 1 and star 2 of the pair respectively.

Column	Heading	Units	Description
1	ipix_1		Identifier
2	raj2000_1	deg	Right Ascension J2000.0, epoch 2000.0
3	dej2000_1	deg	Declination J2000.0, epoch 2000.0
4	e_raepra_1	deg	Mean error in RA*cos(delta) at mean epoch
5	e_deepde_1	deg	Mean error in Dec at mean epoch
6	pmra_1	deg/yr	Proper motion in RA*cos(delta)
7	pmde_1	deg/yr	Proper motion in Dec
8	e_pmra_1	deg/yr	Mean error in pmRA*cos(delta)
9	e_pmde_1	deg/yr	Mean error in pmDE
10	nobs_1		Number of observations used
11	epra_1	yr	Mean Epoch (RA)
12	epde_1	yr	Mean Epoch (Dec)
13	jmag_1	mag	J selected default magnitude from 2MASS
14	e_jmag_1	mag	J total magnitude uncertainty
15	hmag_1	mag	H selected default magnitude from 2MASS
16	e_hmag_1	mag	H total magnitude uncertainty
17	kmag_1	mag	K_s selected default magnitude form 2MASS
18	e_kmag_1	mag	K_s total magnitude uncertainty
19	b1mag_1	mag	B mag from USNO-B, first epoch

20	b2mag_1	mag	B mag from USNO-B, second epoch
21	r1mag_1	mag	R mag from USNO-B, first epoch
22	r2mag_1	mag	R mag from USNO-B, second epoch
23	imag_1	mag	I mag from USNO-B
24	magsurveys_1		Surveys the USNO-B magnitudes are taken from
25	flags_1		Flags
26-50			Columns 1-25 repeated for 2nd star of the pair.
51	Separation	arcsec	Distance between matched objects
52	id		abs(ipix_1-ipix_2)
53	jdiff	mag	jmag_1-jmag_2
54	jk_1	mag	jmag_1-kmag_1
55	jk_2	mag	jmag_2-kmag_2
56	jkdiff	mag	jk_1-jk_2
57	middle		((5*log10(3600*sqrt(pmra_1*pmra_1+pmde_1*pmde_1))))
58	H(J)		jmag_1+middle+5
59	diff_dec		pow(dej2000_1-dej2000_2, 2)
60	diff_ra		raj2000_1-raj2000_2
61	sep	deg	sqrt(diff_dec+(pow(diff_ra*cosDeg(dej2000_1), 2)))
62	sep_AU	AU	Separation*dist
63	sep_SI	m	sep_AU*1.49e11
64	sigpm		(sqrt(pmra_2*pmra_2+pmde_2*pmde_2)/sqrt(e_pmra_2*e_pmra_2+e_pmde_2*e_pmde_2))
65	vel	m/s	(sqrt((6.67e-11*0.8*2e30)/sep_SI))
66	vel_kms	km/s	vel/1000

Figure 4.15   Table headings for the final catalogue, with units and column descriptions.

4.6   SuperCOSMOS

Based on the recommendation of Dr. Nigel Hambly we have applied our selection criteria on the SuperCOSMOS catalogue (Hambly et al., 2001a) for a short comparison against the result from PPMXL.

The majority of the selection criteria shown in Fig 3.7 remained the same when used on the new catalogue, however the following changes were made to the new criteria:

- SuperCOSMOS includes a prediction for whether each source is a star or not. This was used to only include sources expected to be stars.
- R and I magnitudes were used in place of the J and K magnitudes
- One of the PPMXL criteria used the value of 5σ based on the average proper-motion of the catalogue. A new value has been calculated using the average proper-motion from SuperCOSMOS
- New colour cuts were used that better fit the main sequence for the new colours
- A new calculation was performed for the slope of the RPM criteria using the new colours
- An upper RPM limit for the galactic escape velocity was imposed.

The final selection criteria imposed on the SuperCOSMOS catalogue are shown here in Figure 4.16.

```
SELECT TOP 1000000000 *
FROM supercosmos.sources as supercos
Left outer join supercosmos.sources as supercosm
on 1=CONTAINS(POINT('ICRS' , supercos.raj2000, supercos.dej2000),
CIRCLE ('ICRS', supercosm.raj2000, supercosm.dej2000, 0.1))
Where
supercos.meanclass=2
and abs(supercos.objidr2-supercosm.objidr2)>0
and ((abs((supercos.pmra-supercosm.pmra)/power(supercos.e_pmra*supercos.e_pmra+
supercosm.e_pmra*supercosm.e_pmra, 0.5)))<2
and ((abs((supercos.pmde-supercosm.pmde)/power(supercos.e_pmde*supercos.e_pmde+
supercosm.e_pmde*supercosm.e_pmde, 0.5)))<2
and (abs(supercos.raj2000-supercosm.raj2000)*cos(radians(supercos.dej2000))>0.0005 or
abs(supercos.dej2000-supercosm.dej2000)>0.0005)
and supercos.scormagr2>=supercosm.scormagr2
and supercos.scormagr2-supercos.scormagi>0.15 and supercos.scormagr2-supercos.scormagi<0.6
and supercosm.scormagr2-supercosm.scormagi>0.15 and supercosm.scormagr2-
supercosm.scormagi<0.6
and (abs(supercos.pmra/supercos.e_pmra)>5 or abs(supercos.pmde/supercos.e_pmde)>5)
and (abs(supercosm.pmra/supercosm.e_pmra)>5 or abs(supercosm.pmde/supercosm.e_pmde)>5)
and supercos.scormagr2+5*log10(0.0000001+3600*power(supercos.pmra*supercos.pmra+
supercos.pmde*supercos.pmde, 0.5))+5>8.4+15*(supercos.scormagr2-supercos.scormagi)
and supercosm.scormagr2+5*log10(0.0000001+3600*power(supercosm.pmra*supercosm.pmra+
supercosm.pmde*supercosm.pmde, 0.5))+5>8.4+15*(supercosm.scormagr2-supercosm.scormagi)
and supercos.scormagr2+5*log10(0.0000001+3600*power(supercos.pmra*supercos.pmra+
supercos.pmde*supercos.pmde, 0.5))+5<10.9+15*(supercos.scormagr2-supercos.scormagi)
and supercosm.scormagr2+5*log10(0.0000001+3600*power(supercosm.pmra*supercosm.pmra+
supercosm.pmde*supercosm.pmde, 0.5))+5<10.9+15*(supercosm.scormagr2-supercosm.scormagi)
and abs(sin(radians(supercos.dej2000))*cos(radians(62.87))-cos(radians(supercos.dej2000))*
sin(radians(supercos.raj2000-282.86))*sin(radians(62.87)))>0.2588
and (supercos.raj2000>90 or (supercos.dej2000>-60 or supercos.dej2000<-80))
and (power(supercos.pmra*pmra+supercos.pmde*supercos.pmde,0.5)>0.000044445)
```

Figure 4.16   Selection criteria imposed on the SuperCOSMOS catalogue based on those

created in Ch. 3.

These selection criteria produced a catalogue of 516 candidate CPM halo binary pairs,

compared to the 17,500 pairs from the PPMXL catalogue; though due to the number of issues

identified with PPMXL, the SuperCOSMOS catalogue is expected to be much more reliable.

Following similar steps to those performed on the PPMXL catalogue, a short analysis was performed on this new catalogue to compare it to the catalogue we produced in Ch. 4.5.
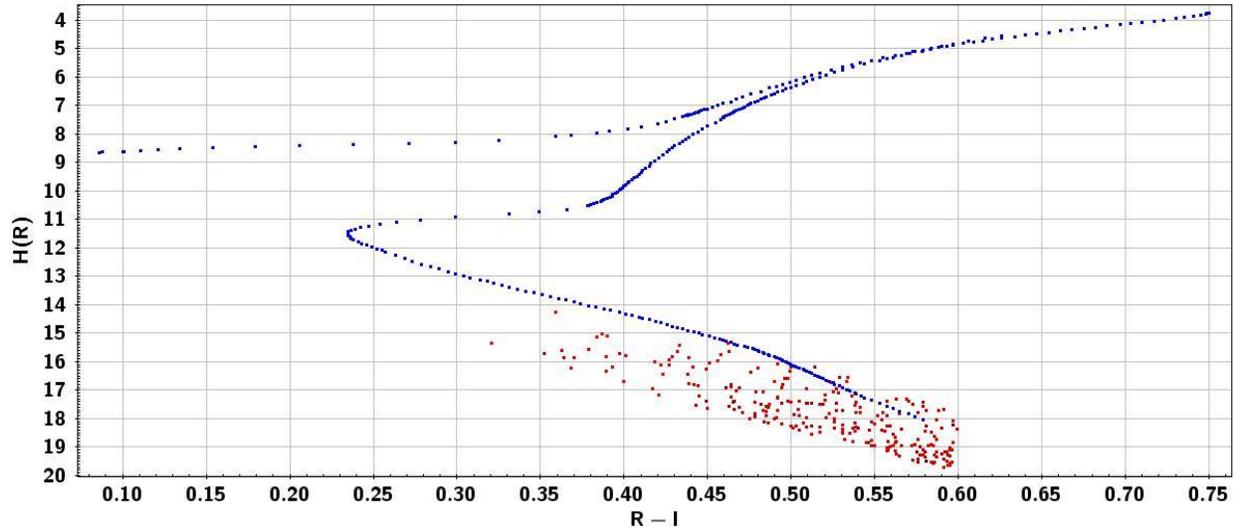
Figure 4.17   RPM plot for the selected SuperCOSMOS data, including Padova isochrone for a typical halo star (*Z*=0.0001, *age*=12 Gyr, $v_\perp = 200 \text{ kms}^{-1}$).

Due to the limited sample produced by the selection criteria it is difficult to tell if there is much correlation in Figure 4.17, though it is evident that the plot is slightly denser for larger $(R - I)$ values. As there are likely to be few very low metallicity stars in this catalogue, it is understandable that not many sources are found to match perfectly with the Padova isochrone.
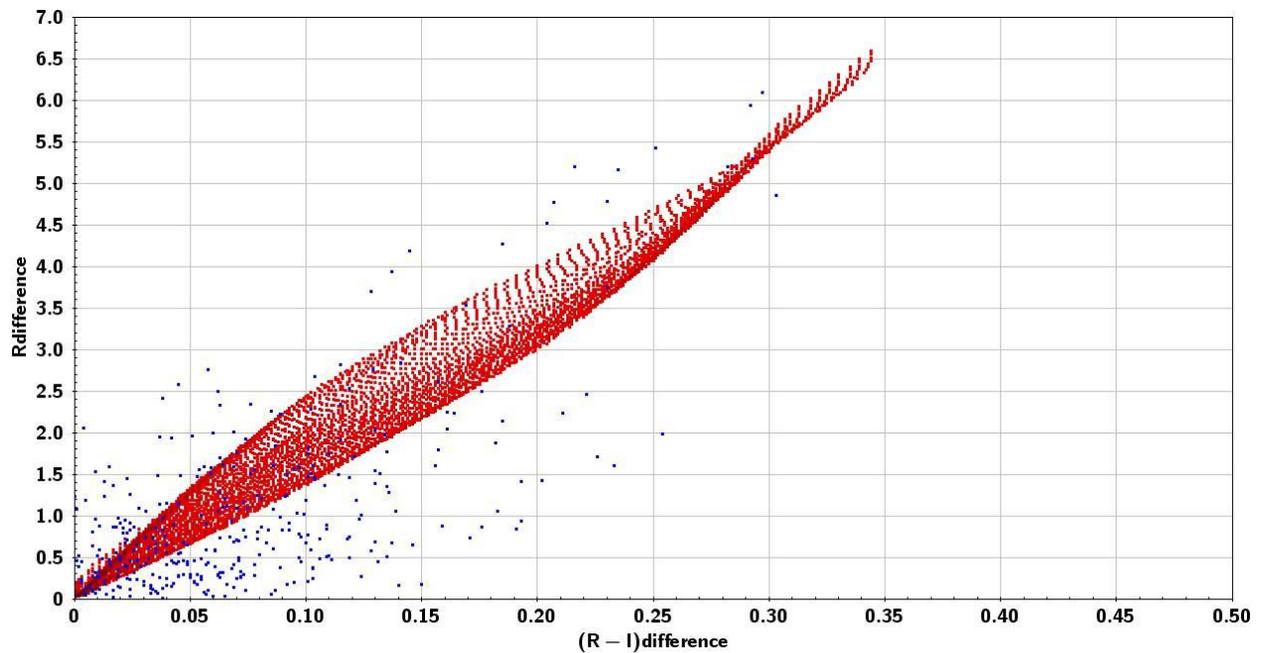
Figure 4.18   Theoretical binaries using the Padova isochrones as detailed in Ch. 4.3 with the selected SuperCOSMOS data in blue.

Figure 4.18 is encouraging as loose correlation to the theoretical main-sequence pairings is apparent, and much more evident than was produced by the PPMXL catalogue (Fig 4.4). Though a large portion of the catalogue is outside the red region shown, these stars are likely pairs where only one of the stars is on the main-sequence.
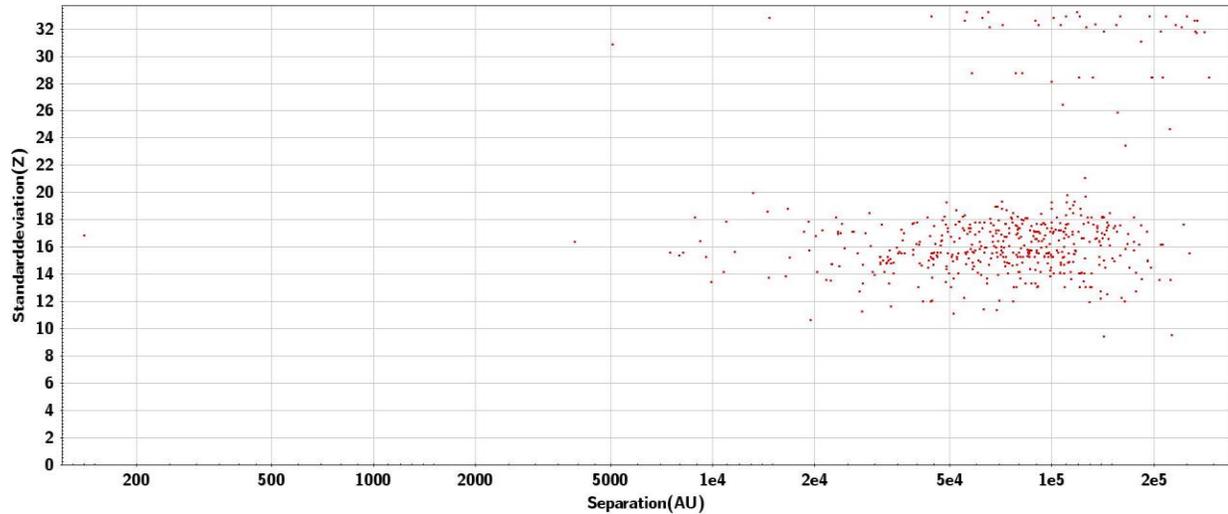
Figure 4.19   Significance of the proper motion of star 2 (number of standard deviations) vs the physical separation (AU) of the pair.

The SuperCOSMOS equivalent to Fig. 4.14, Fig. 2.19, has a couple of interesting features; notably the apparent gap between ~20 to 26 standard deviations. It is unclear what the source of this feature is and further analysis would be required to uncover its cause. Secondly of note is that using the constraints of $Z > 10$ or Sep $< 1 \times 10^4$ AU from Fig 4.14, only 2 sources are excluded.

Based on the short analysis of the SuperCOSMOS catalogue's use in identifying CPM halo binaries, it would appear that the data are significantly more reliable than those produced by the PPMXL catalogue, however the reduced number of sources would mean fewer low metallicity halo binaries would be found compared to the final catalogue in Ch. 4.5. The list of 514 sources could be added to the likely candidate list produced from the PPMXL catalogue for use in prospective future work.

5.0 Identification of Candidate Halo Giants

During the early stages of creating appropriate selection criteria for the catalogue, a prominent feature was noticed in a RPM plot which appeared to be caused by the inclusion of a large number of halo giants.

This feature contained roughly 600,000 stars, of which a large number were hoped to be halo giants. Halo giants are quite rare, so the possibility of having found such a large quantity in the data was worth looking into for a side project.

Using Padova isochrones, it was determined that the feature does coincide with the giant branch of a star in the halo. Figure 5.1 shows Padova isochrones for $\log(Age/\text{yr}) = 10.05$ typical halo stars with $Z = 0.00001$ for both $v_\perp = 100$ and 200 km s^{-1} which coincides with some of the data. However, a range of isochrones of differing metallicities, ages and transverse velocities was also included; these alternatives include thick disk ($Z = 0.004$) and solar ($Z = 0.017$) metallicities and more moderate transverse velocities ($v_\perp = 25 - 50$ kms^{-1} and $v_\perp = 10 - 20$ kms^{-1} respectively) which occupy similar regions of the RPM diagram to the typical halo stars, as shown in Fig. 5.1.

Because of this overlap with much more common stars, the number of actual halo giants in the data will be much lower than first hoped. To separate the halo giants from the other stars, spectroscopic data would be required, but this was outside the scope of the project so was not pursued.
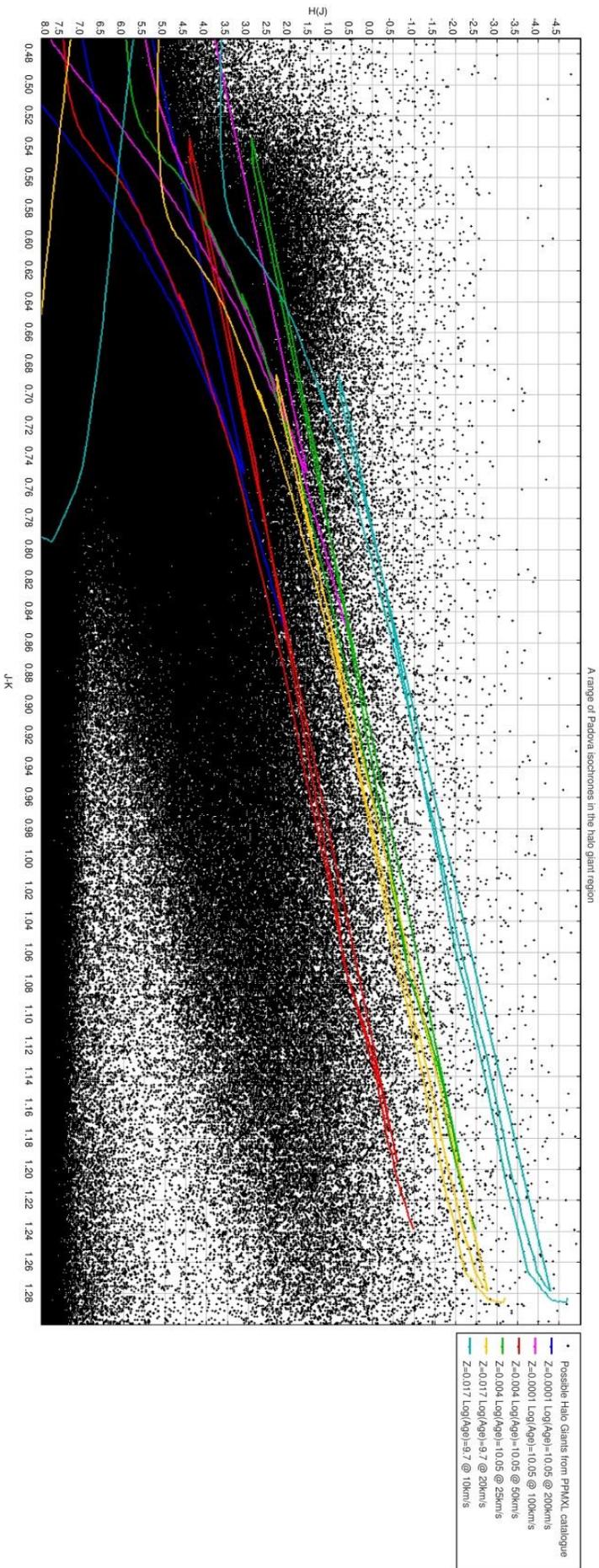
Figure 5.1   A selection of Padova isochrones in the halo giant region, showing the contamination present from non-halo stars.

6.0 Future Work

Due to the low quality and poor reliability of the candidates we produced, based on the observed inconsistencies between proper-motion data given by the PPMXL catalogue and that of multiple outside sources, the next step would be to identify a more reliable source for creating a catalogue.

As the problems experienced using the PPMXL catalogue appear to stem from USNO-B1, the second choice based on the analyses done in Ch. 2 cannot be used. From the work done in Ch. 2, the next best choice would be LSPM.

LSPM catalogue has improved accuracy compared to the PPMXL and USNO-B1 catalogues, but was rejected in the original analysis due to having a much smaller number of sources. While the resulting catalogue created from LSPM would be much smaller than the one we produced, it should hopefully be much more accurate.

The selection criteria defined in Ch. 3 should produce reliable results when used to query the LSPM catalogue, but due to the lack of correlation found in the final catalogue we produced from PPMXL, it would be prudent to analyse the criteria again to ensure non-halo stars are being removed fully.

Another consideration would be to make use of the SuperCOSMOS catalogue. It was briefly shown in Ch. 4.6 that though few low metallicity pairs would be found in this catalogue, any that were identified would be on high quality and sufficient for some of the planned future work.

After this point, assuming a catalogue of reliable halo CPM pairs was created using LSPM, the original planned work could be implemented.

- Obtain additional, improved photometry for the new catalogue, allowing any remaining disk stars to be separated from the halo stars. Additional photometry could be used to give early metallicity estimates and allow preferential candidates to be chosen.

- SDSS includes some spectroscopy which can be used to attempt to determine the metallicity of the binaries in the new catalogue. If spectroscopic data were not available, a spectroscopic study can be undertaken to obtain additional data. This would mean a brightness limit cut may need to be considered. An estimate for this would be $i = 18$ for intermediate resolution and $i = 15$ for high resolution.

- The metallicity distribution of globular clusters is shown to cut off at $[Fe/H] = -2.4$ (Kraft & Ivans, 2003) which is much higher than that of single field stars, $[Fe/H] = -4.1$ (Yong et al., 2012). The planned future work for the project was to attempt to use any metal-poor binaries from the new catalogue to investigate the causes behind the lower metallicity distribution of globular clusters, and to provide ages by isochrone fitting to CPM pairs in the field-star population.

- Assess the distribution of separations of stars in CPM pairs and investigate their origins and the stellar density of the environments in which they formed.

- Assess which pairs may be valuable for investigating the mass dependence of stellar evolutionary phenomena such as lithium depletion and turbulent diffusion (Aoki et al., 2012).

An additional direction that could be taken would be to attempt to observe the 528 and 514 preferred candidates shown in Fig. 4.14 and Fig 4.19 respectively. These sources have extremely significant proper-motion values, and should likely be genuine CPM binary pairs. Though, due to the observed problems in the USNO-B1 and PPMXL catalogues, it is possible that a number of these candidates are fictitious. Whether it is preferential to sort through this list of candidates or attempt to create a new list using a secondary catalogue like LSPM is debateable.

Some considerations for future work to be undertaken using either direction would be to determine probabilities for the reliability of candidates based on their proper-motion differences, separations and photometry. An example of this was touched upon in Ch. 3.5 regarding the probabilities of false pairings due to line of sight based on the separation

between prospective pairings. Calculating the probability of these chance pairings can be used to determine the legitimacy of the pairs in our catalogue.

Another consideration would be the implementation of future surveys in improving the data used to create the catalogue:

- Gaia's objective is to precisely measure the positions, distances, movements and changes in magnitude for a billion stars[8]. This will provide much more accurate data than was available for this project and could be used to create a reliable CPM halo binary catalogue.
- PanSTARRS[9] could be used to obtain accurate data with multiple visits to sources, allowing it to find sources with high proper-motions which could be used for a future catalogue.
- By imaging the entire night sky repeatedly, accurate proper-motions could be used from the Large Synoptic Survey Telescope (LSST) in the future[10] as well as accurate positions. The accuracy of this survey will surpass all current catalogues and would therefore be incredibly useful for attempting to find CPM halo binaries.

---

[8] http://sci.esa.int/gaia/47354-fact-sheet/
[9] http://pan-starrs.ifa.hawaii.edu/public/science-goals/stars-galaxy.html
[10] http://www.lsst.org/science

7.0   Conclusions

The aim of the project was to create a catalogue of common-proper-motion halo stars from existing catalogues. This was done by tailoring a number of selection criteria, designed to produce only stars which met the physical requirements of typical halo binaries, and apply it to PPMXL, the proper-motion catalogue chosen for the study, which resulted in a list of roughly 17,500 CPM halo binary candidates, which has been shown to contain a number of previously identified CPM binaries.

This catalogue was constrained further with the use of Padova isochrones, allowing for an estimation of the range in which two metal-poor halo stars on the main sequence would be found. This resulted in a smaller, more reliable catalogue of around 2,326 pairs. From this catalogue, a list of 318 high priority targets has been identified, with extremely significant $\left(> 10\sigma_\mu \right)$ proper-motions.

During our analysis of the larger (17,500 source) catalogue, it was revealed from a comparison between the proper-motions in our catalogue with a number of outside sources (rNLTT, LSPM, Hipparcos, DSS and more) that a large number of our sources have incorrect data. We have found that a large number of problems, arising from the methods used to create the original USNO-B1 catalogue have translated through to our catalogue through PPMXL, which was based on the USNO-B1 catalogue, causing a number of errors and inconsistencies with the data, which has drastically lowered the credibility of our proposed catalogue of CPM halo binaries. Multiple problems were also identified, primarily a 'crosshair' feature appearing in fields, whereby diffraction spikes from bright $(J < 11.5)$ sources had been converted into multiple, non-existent fainter sources in a crosshair pattern surrounding the bright star. These fictitious sources had sometimes been given large, erroneous proper-motions and appeared in our larger catalogue. An additional problem which also featured in fields containing bright sources was where the original USNO-B1 catalogue has identified multiple sources of similar magnitudes, in roughly the same location for a single bright source. The example provided in Ch. 4.4.4 shows 5 bright sources in place of 2 genuine sources.

Some smaller problems that have been identified are the dense brickwork pattern in the final catalogue caused by the plate boundaries of the original photographic plates and a proper motion spike where an increased number of sources are found to have proper-motions in the direction of positive RA.

Finally there is a severe lack of any of the colour-magnitude correlation that would have been expected from a catalogue consisting of main-sequence CPM halo binaries. When compared with theoretical isochrones, none of the expected features are present, which is a big indication that the 17,500 star catalogue does not contain a majority of the stars we intended it should.

Due to the low reliability of the results of our final catalogue, its data cannot be trusted for use in any of the further analysis or future work which was originally planned. The methods used in the creation of the selection criteria are nevertheless expected to be much more reliable, and could therefore be used in attempts to obtain the originally desired catalogue from other source catalogues, such as SuperCOSMOS, as we did, or LSPM, and as a shortlist for further observations to identify genuine halo CPM binaries

8.0 Appendix

Standard Deviations (Z)	Number of Sources (N) $(\mu/\epsilon_\mu \geq Z)$	ln(N)
0.0	10000	9.21
0.5	9840	9.19
1.0	9403	9.14
1.5	8637	9.06
2.0	7623	8.94
2.5	6622	8.80
3.0	5712	8.65
3.5	5080	8.53
4.0	4591	8.43
4.5	4207	8.34
5.0	3854	8.26
5.5	3584	8.18
6.0	3367	8.12
6.5	3155	8.06
7.0	2977	7.99
7.5	2804	7.93
8.0	2651	7.88
8.5	2491	7.82
9.0	2361	7.77
9.5	2229	7.71
10.0	2126	7.66
10.5	2039	7.62
11.0	1983	7.59
11.5	1926	7.56
12.0	1882	7.54
12.5	1851	7.52
13.0	1825	7.51
13.5	1804	7.50
14.0	1780	7.48
14.5	1754	7.47
15.0	1733	7.46

Table 8.1   The table accompanying Figure 3.1 showing the number of catalogue sources with proper-motions (μ) higher than Z times the proper-motion error (ϵ_μ)

9.0   References

Ahn C. P., Alexandroff R., Allende Prieto C., Anderson S. F., Anderton T., Andrews B. H., Aubourg É., Bailey S., Balbinot E., Barnes R., et al. 2012, ApJS, 203, 21

Ahn C.P., Alexandroff R., Allende Prieto C., Anders F., Anderson S. F., Anderton T., Andrews B. H., Aubourg É., Bailey S., Bastien F. A., et al. 2014, ApJS, 211, 17

Allen C., Poveda A., Hernández-Alcántara A., 2007, in Hartkopf W. I., Harmanec P., Guinan E. F., eds, IAU Symposium Vol. 240 of IAU Symposium, Halo Wide Binaries and Moving Clusters as Probes of the Dynamical and Merger History of our Galaxy. pp 405–413

Aoki W., Ito H., Tajitsu, A., 2012, ApJ, 751, L6

Asplund M., Grevesse N., Sauval A.J., 2006, CoAst, 147, 76-79

Bakos G. Á., Sahu K. C., Németh P., 2002, ApJS, 141, 187

Bertelli G., Girardi L., Marigo P., Nasi E., 2008, A&A, 484, 815

Blaauw A., 1999, AP&SS, 267, 45-54

Chanamé J., Gould A., 2004, ApJ, 601, 289

Cox A., 2000, Allen's Astrophysical Quantities, 4th ed, , Springer Science & Business Media

Gould A., 2003, AJ, 126, 472

Gould A., Morgan C. W., 2003, ApJ, 585, 1056

Hambly N. C., MacGillivray H. T., Read m. A., Tritton S. B., Thompson E. B., Kelly B. D., Morgan D. H., Smith R. E.,Driver S. P., Williamson J., et al., 2001, MNRAS, 326, 1279-1294

Hambly N. C., Davenhall A. C., Irwin M. J., MacGillivray H. T., 2001, MNRAS, 326, 1315-1327

Hambly N. C., Irwin M. J., MacGillivray H. T., 2001, MNRAS, 326, 1295-1314

Hertzsprung, E., 1905, Zeitschrift Fur Wissenschaftliche Photographie, 3, 442-449

Jofré P., Weiss A., 2011, A&A, 533, A59

Kraft R. P., Ivans I. I., 2003, PASP, 115, 143-169

Lang K. R., 1980, Sci, 207, 174

Lépine S., 2011, in Johns-Krull C., Browning M. K., West A. A., eds, 16th Cambridge Workshop on Cool Stars, Stellar Systems, and the Sun Vol. 448 of Astronomical Society of the Pacific Conference Series, Cool Stars in Wide Binaries: 23,000 Common Proper Motion Doubles from the SUPERBLINK Proper Motion Survey. p. 1375

Lépine S., Shara M. M., 2005, VizieR Online Data Catalog, 1298, 0

Luyten W. J., 1922, PASP, 34, 156

Luyten W. J., 1922, PASP, 34, 54

Luyten W. J., 1979a, VizieR Online Data Catalog, 1087, 0

Luyten W. J., 1979b, VizieR Online Data Catalog, 1098, 0

Monet D. G., Levine S. E., Canzian B., et al. 2003, AJ, 125, 984

Quinn D. P., Wilkinson M. I., Irwin M. J., Marshall J., Koch A., Belokurov V., 2010, in Prša A., Zejda M., eds, Binaries - Key to Comprehension of the Universe Vol. 435 of Astronomical Society of the Pacific Conference Series, Dark Matter Constraints from Wide Halo Binary Stars. p. 453

Roeser S., Demleitner M., Schilbach E., 2010, AJ, 139, 2440

Ryan S.G., 1992, AJ, 104, 1144-1155

Ryan S. G., Deliyannis C. P., 1998, ApJ, 500, 398

Salim S., Gould A., 2003, Astrophys.J., 582, 1011-1031

Sandage, A., 1953, Astrophys.J., 58, 61-75

Schlesinger K. J., Johnson J. A., Rockosi C. M., Lee Y. S., Morrison H. L., Schönrich R., Prieto C. A., Beers T. C., Yanny B., Harding P., et al., 2012, ApJ, 761, 160

Skrutskie et al., R. M.,2006, AJ, 131, 1163

Strobel N., 2013, Astronomy Notes (2013 edition), Available from: www.astronomynotes.com/index.html [Accessed 24/6/2015]

Strömberg G., 1939, AJ, 89, 10

Tissera P. B., Scannapieco C., 2014, MNRAS, 445, 21-25

Titov, O., 2010, MNRAS, 407, 46-48

Yong D., Norris J. E., Bessell M. S., Christlieb N., Asplund M., Beers T. C., Barklem P. S., Frebel A., Ryan S. G., 2012,ApJ, 762, 27